Figure 36. Plots of selected results of the high NO_x lumped molecule surrogate reactivity experiments for **m-xylene**
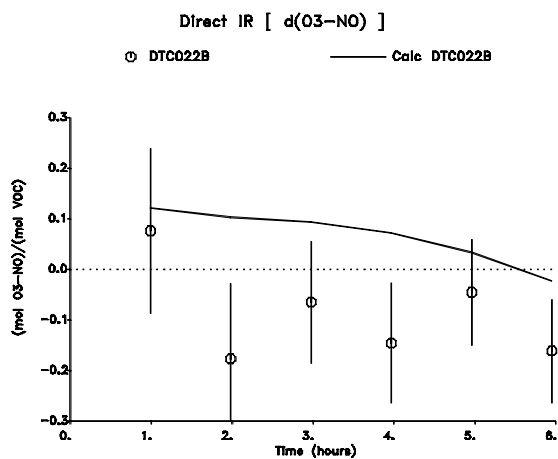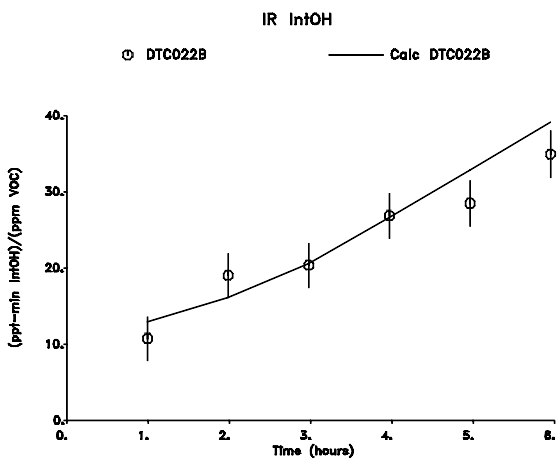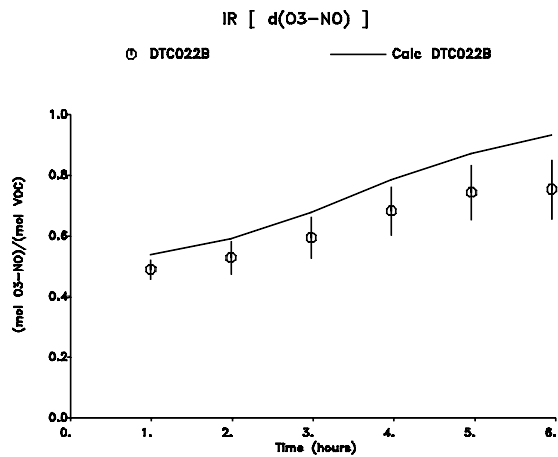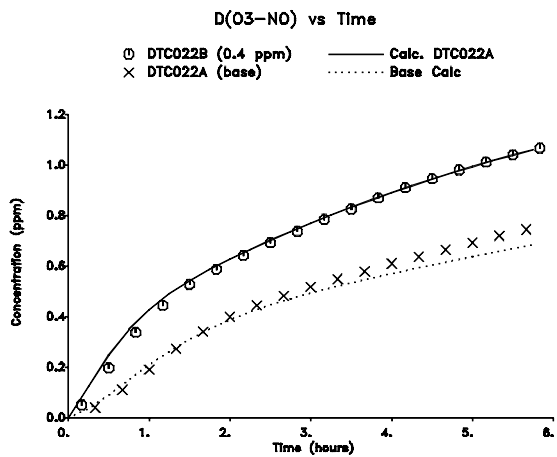
Figure 37. Plots of selected results of the high NO_x lumped molecule surrogate reactivity experiment for **formaldehyde**
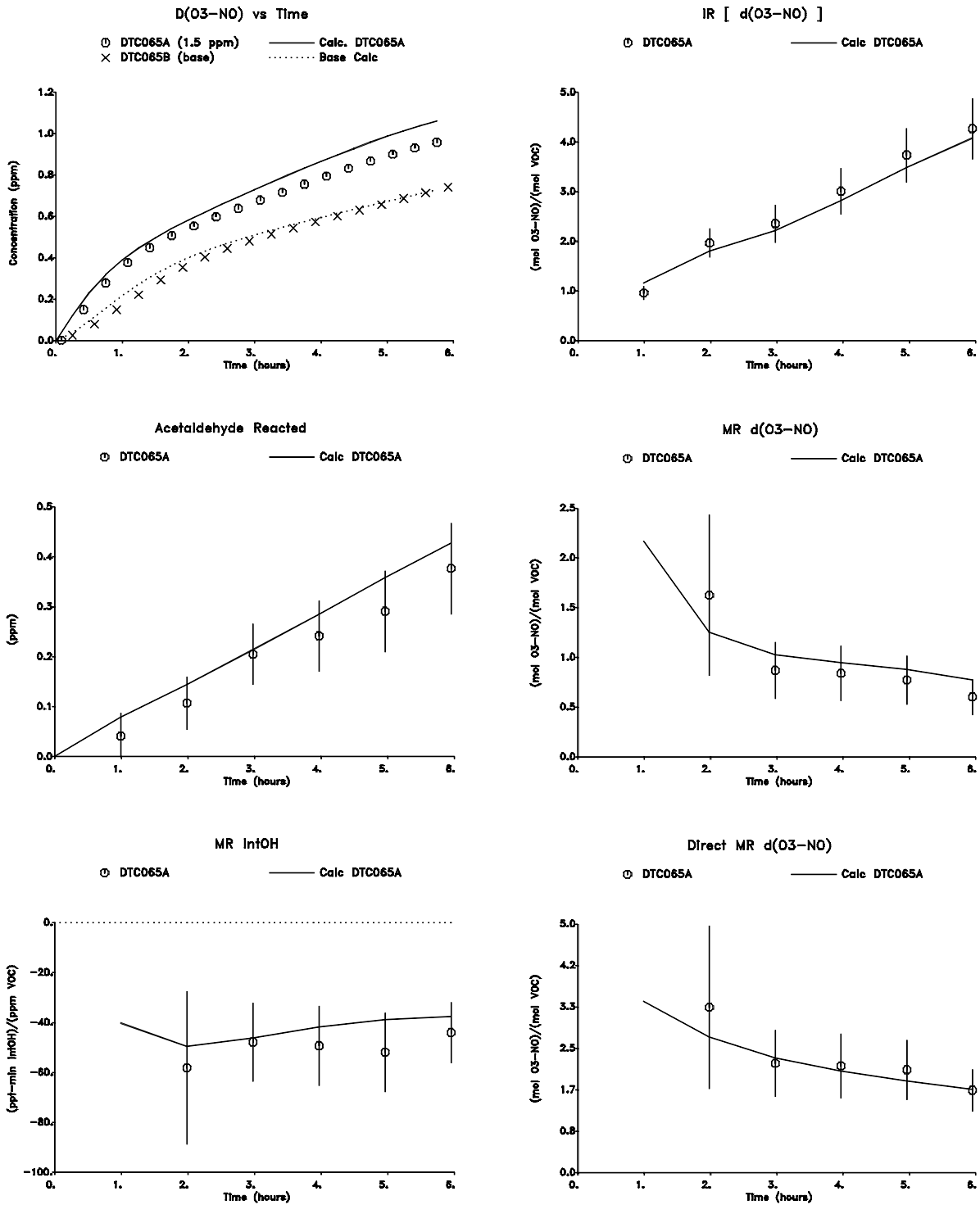
Figure 38. Plots of selected results of the high NO_x lumped molecule surrogate reactivity experiment for **acetaldehyde**

For most VOCs, the reactivities with respect to $d(O_3-NO)$ tended to be more dependent on reaction time in the low NO_x experiments than was the case under thehigher NO_x conditions. This is presumably because the NO_x conditions change significantly with time in the run, with the experiment having sufficient NO_x to promote rapid O_3 formation in the first hour or so, but then becoming NO_x-limited

by the end of the run. Although both carbon monoxide and n-butane had positive incremental $d(O_3-NO)$ reactivities which were essentially constant throughout the experiments their mechanistic reactivities decreased with time. This is because the amounts reacted increased with time. However, their mechanistic reactivities were still significantly positive at the NO_x-limited end of the experiment. Octane was unique in that its incremental and mechanistic $d(O_3-NO)$ reactivities tended to increase with time, being slightly negative initially, and then becoming significantly positive by the end of the run. In the case of acetaldehyde, the $d(O_3-NO)$ reactivities were initially slightly negative, became more negative until around the middle of the run, and then became slightly less negative. For all the other VOCS, the $d(O_3-NO)$ reactivities (both mechanistic and incremental) tended to decrease with time, i.e., as the conditions became more NO_x-limited. In the case of the olefins and formaldehyde, the $d(O_3-NO)$ reactivities were significantly positive at the beginning, but approached zero or (for trans-2-butene) became slightly negative by the end of the run. In the case of the aromatics, the $d(O_3-NO)$ reactivities were significantly positive initially, but became significantly negative as conditions became NO_x-limited. This behavior for the aromatics is expected based on other experimental (e.g., Carter and Atkinson, 1987) and modeling (Carter and Atkinson, 1989) studies of these compounds.

All the VOCs studied were found to have much more negative effects on integrated OH radical levels under NO_x-limited conditions than was observed in the high NO_x experiments. For example, CO, which had almost no effect on IntOH in the high NO_x experiments, had definite negative IntOH reactivities in these low NO_x runs. Even alkenes and aromatics, which significantly positive effects on radicals under high NO_x conditions, tended to significantly inhibit OH radicals by the end of these experiments. However, trans-2-butene and the aromatics, the strongest radical initiators under high NO_x conditions, had significantly positive effects on radicals around the beginning of the experiments, when NO_x was still present. In terms of magnitude of IntOH inhibition on a per molecule reacted basis, the ordering was CO ≈ ethene < propene < trans-2-butene ≈ benzene ≈ toluene ≈ m-xylene < n-butane < acetaldehyde ≈ n-octane. This is quite different than their ordering of IntOH reactivities under high NO_x conditions. (On a per carbon reacted basis, the inhibition by acetaldehyde was much greater than all other VOCs studied.) Although the IntOH reactivity for formaldehyde was found to be always positive in these low NO_x experiments, the magnitude of the IntOH reactivity was far less than observed in the higher NO_x runs.
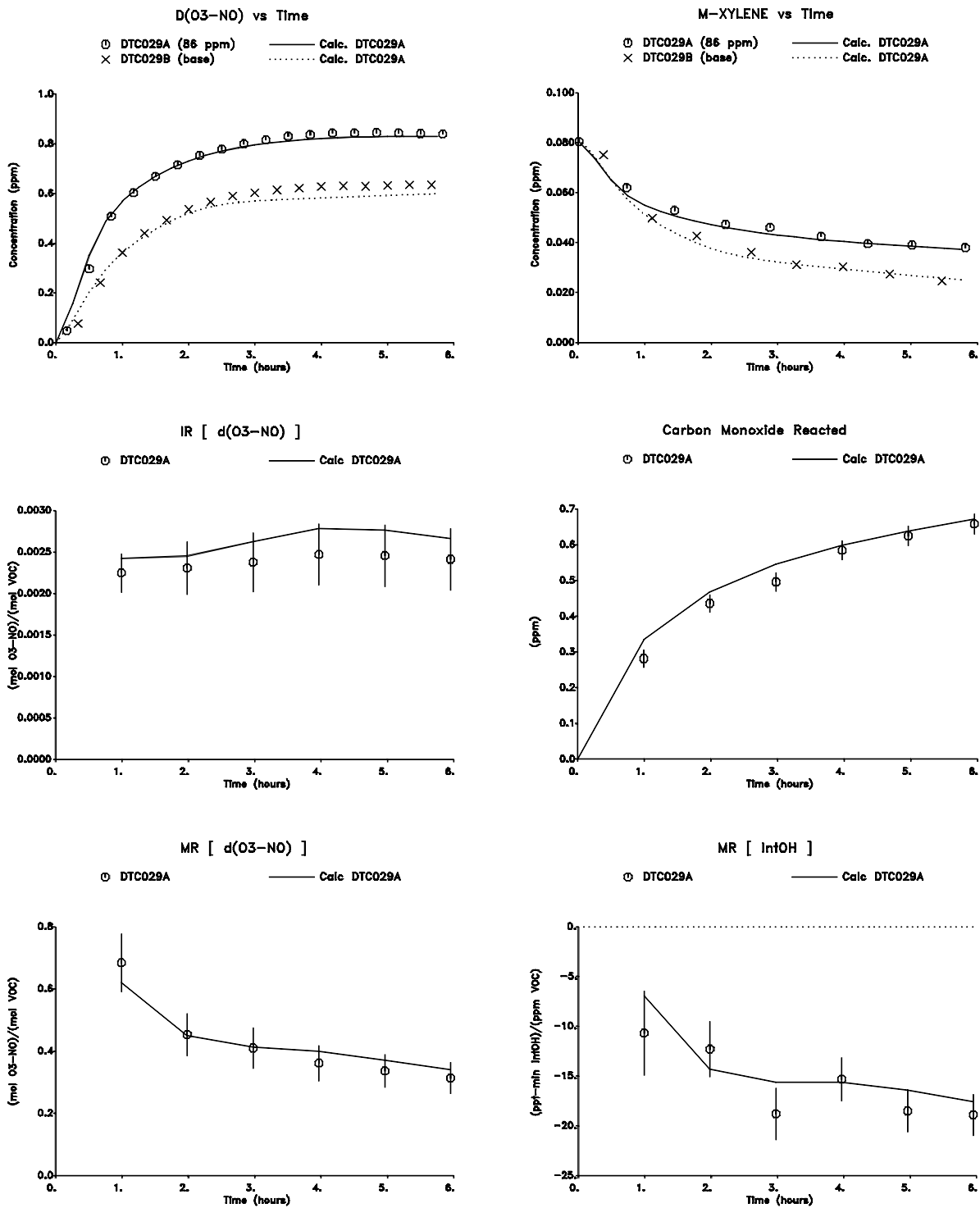
Figure 39. Plots of selected results of the low NO_x lumped molecule surrogate reactivity experiment for **carbon monoxide**
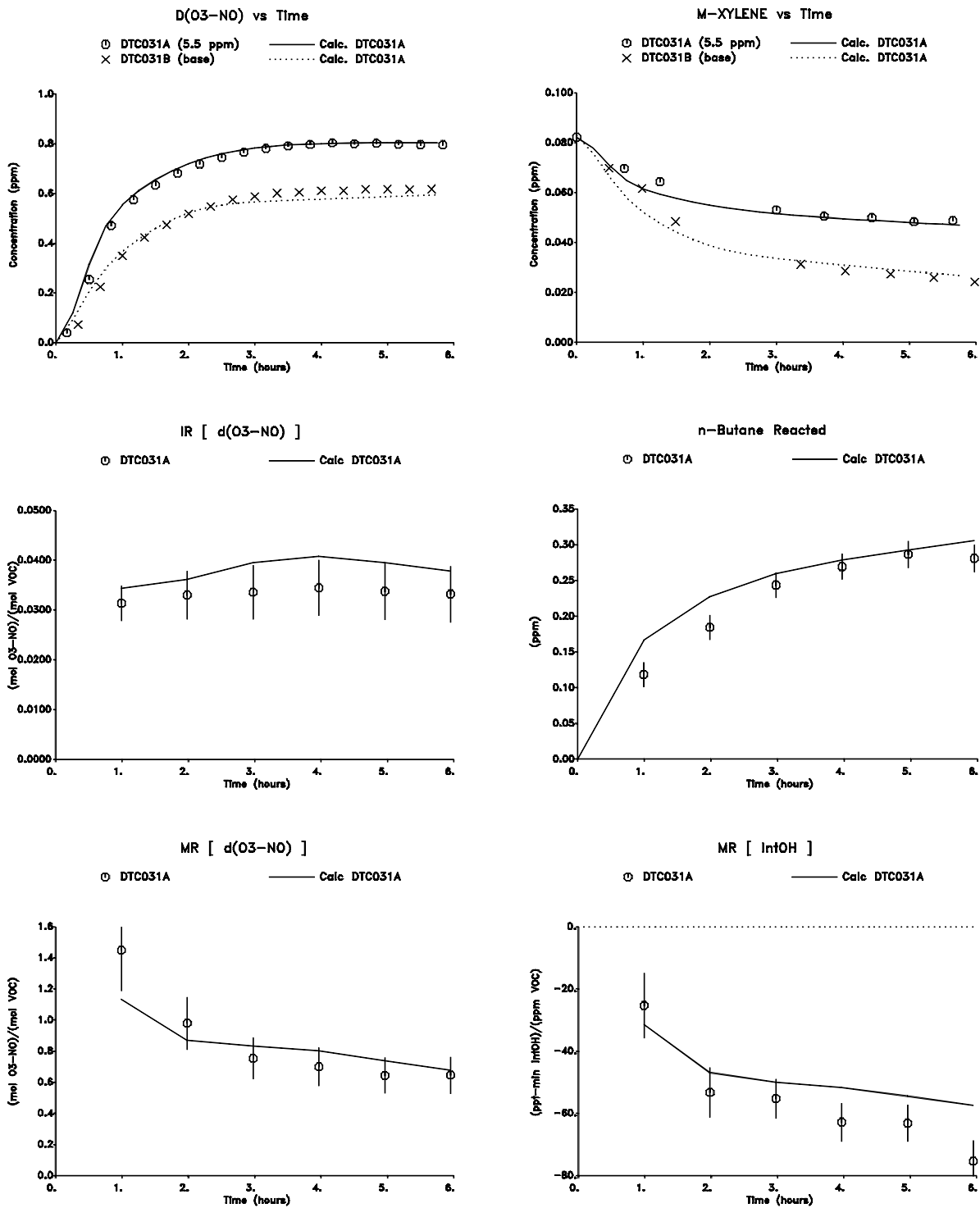
Figure 40. Plots of selected results of the low NO$_x$ lumped molecule surrogate reactivity experiment for **n-butane**
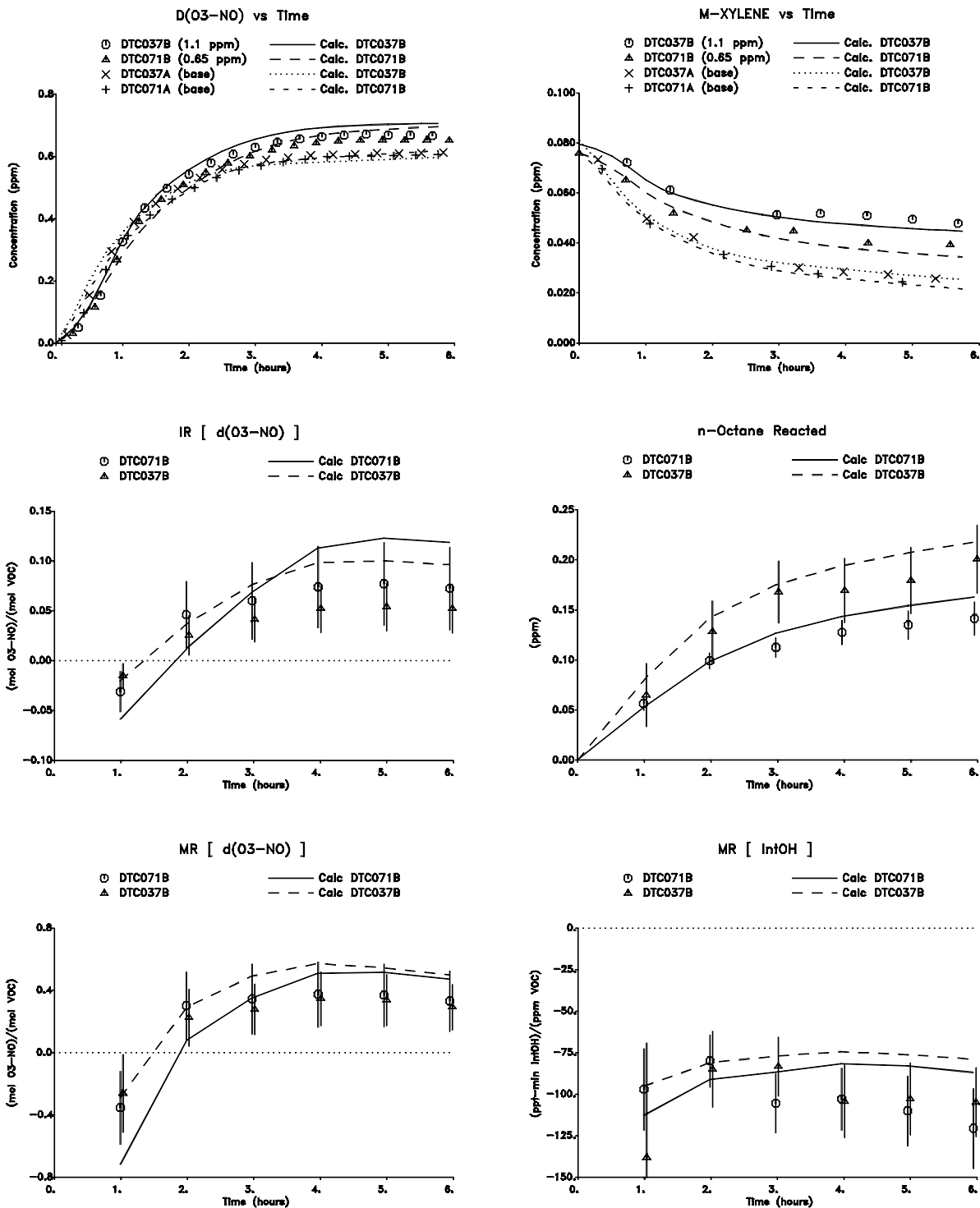
Figure 41. Plots of selected results of the low NO_x lumped molecule surrogate reactivity experiments for **n-octane**

D(O3–NO) vs Time

○ DTC038A (0.66 ppm) —— Calc. DTC038A
✕ DTC038B (base) ······ Calc. DTC038A

M–XYLENE vs Time

○ DTC038A (0.66 ppm) —— Calc. DTC038A
✕ DTC038B (base) ······ Calc. DTC038A

IR [d(O3–NO)]

○ DTC038A —— Calc DTC038A

Ethene Reacted

○ DTC038A —— Calc DTC038A

MR [d(O3–NO)]

○ DTC038A —— Calc DTC038A

MR [IntOH]

○ DTC038A —— Calc DTC038A
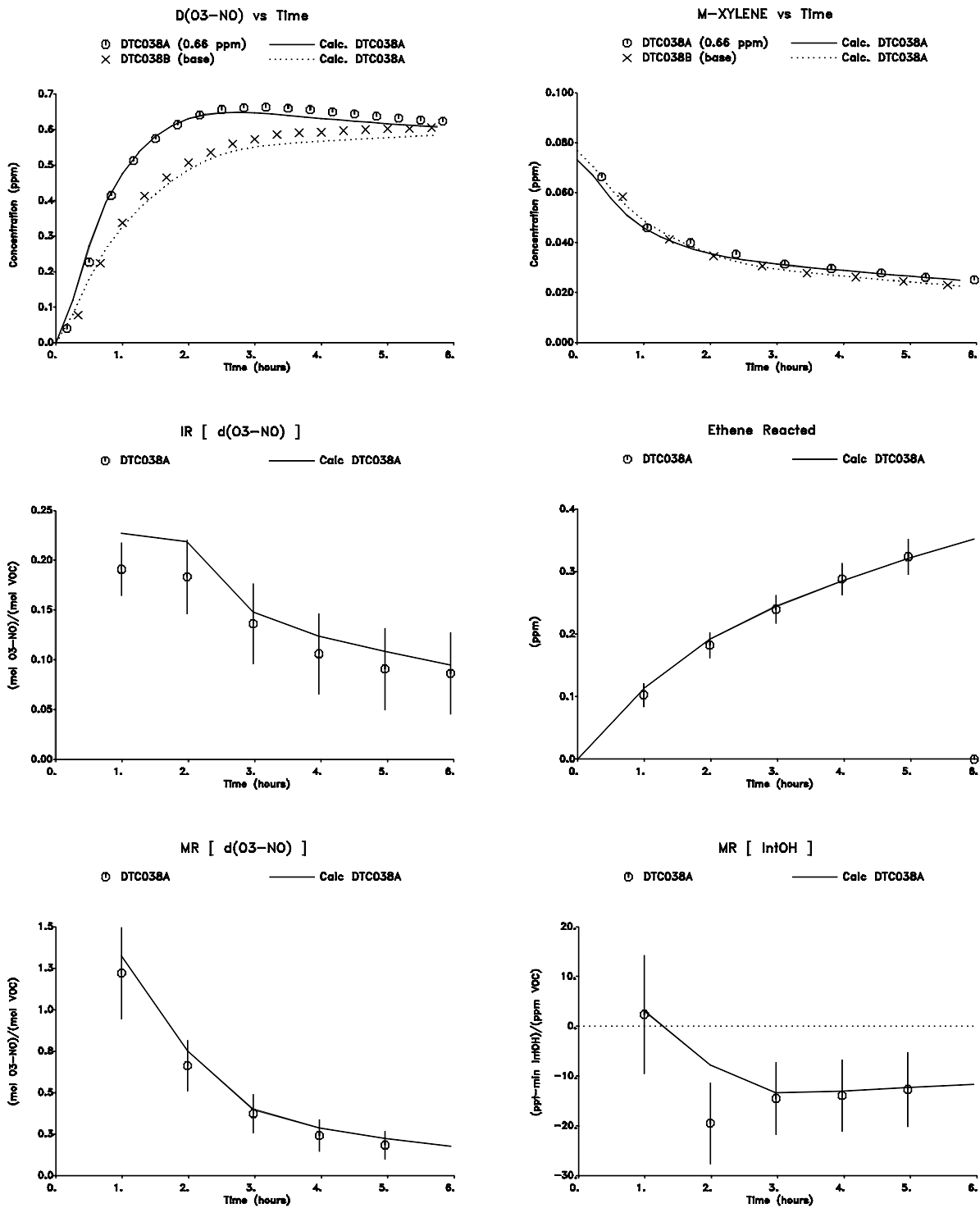
Figure 42. Plots of selected results of the low NO$_x$ lumped molecule surrogate reactivity experiment for **ethene**
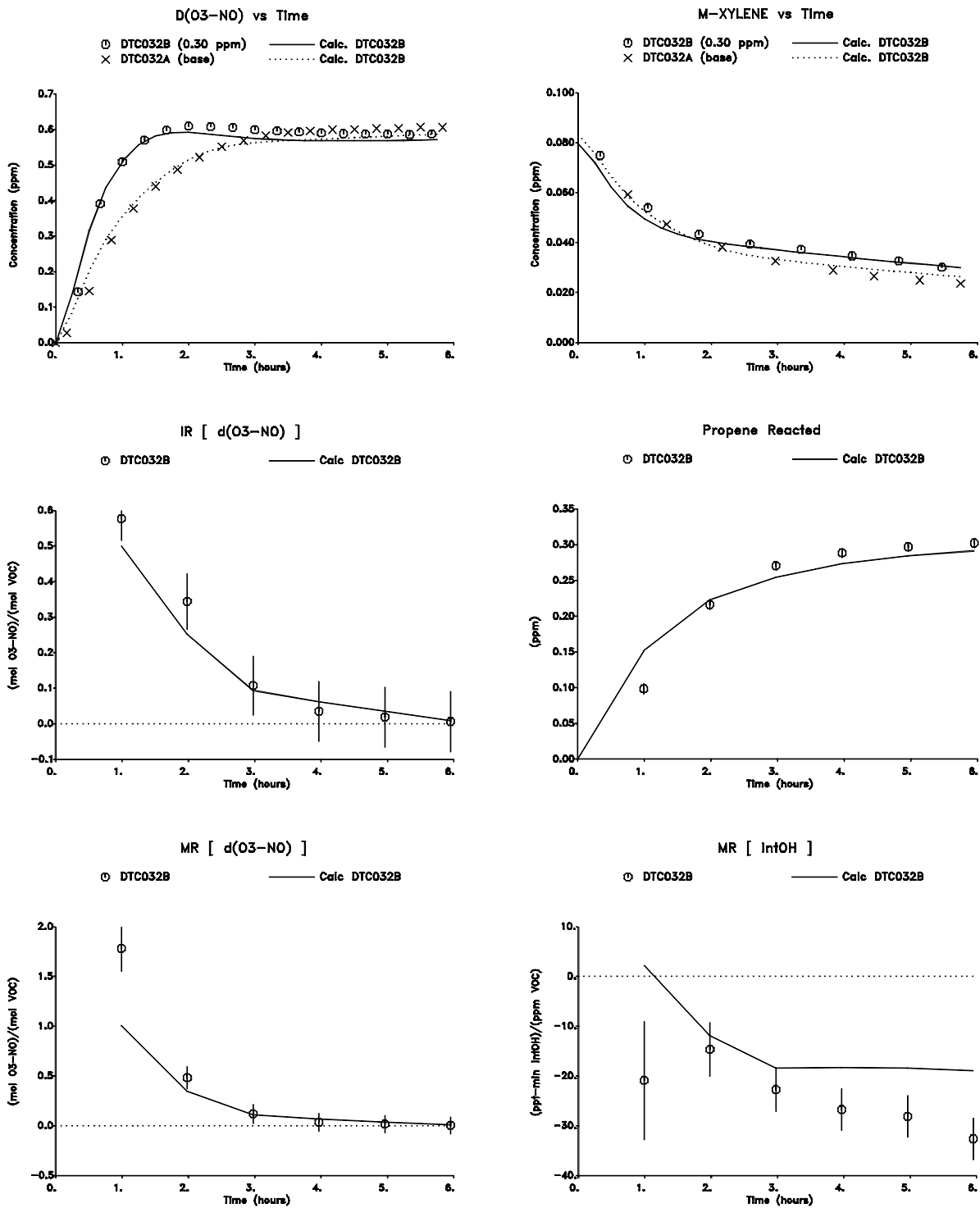
Figure 43. Plots of selected results of the low NO_x lumped molecule surrogate reactivity experiment for **propene**

D(O3-NO) vs Time

- DTC033A (0.16 ppm) ——— Calc. DTC033A
- × DTC033B (base) ········ Calc. DTC033A

M-XYLENE vs Time

- DTC033A (0.16 ppm) ——— Calc. DTC033A
- × DTC033B (base) ········ Calc. DTC033A

IR [d(O3-NO)]

- DTC033A ——— Calc DTC033A

trans-2-Butene Reacted

- DTC033A ——— Calc DTC033A

IR [IntOH]

- DTC033A ——— Calc DTC033A
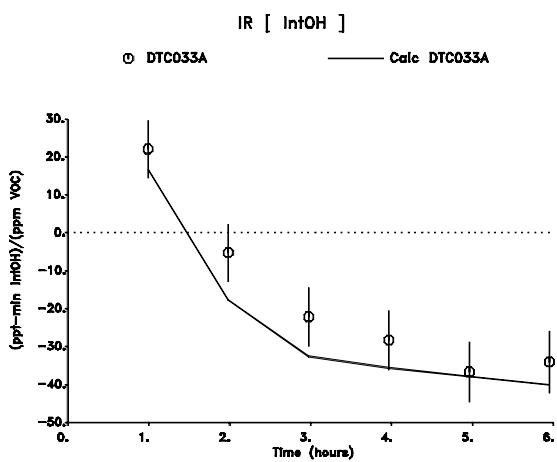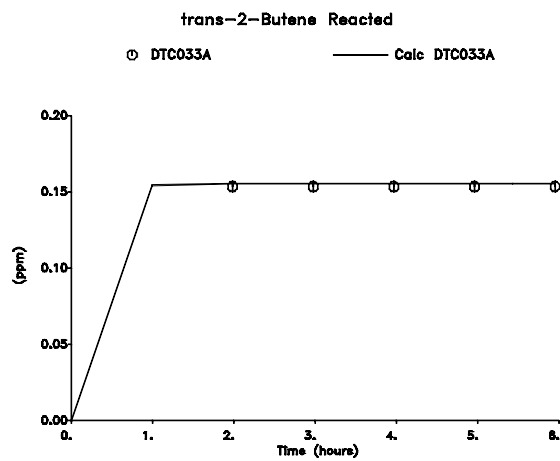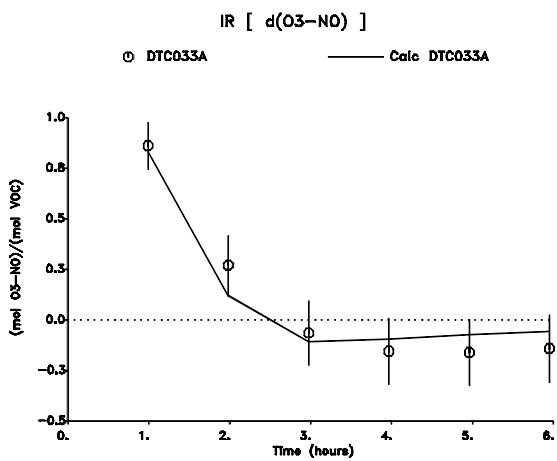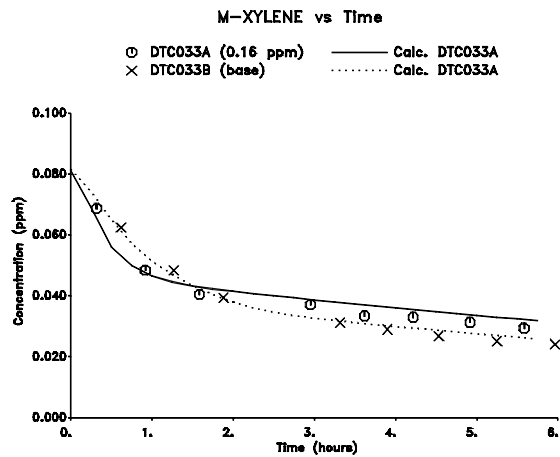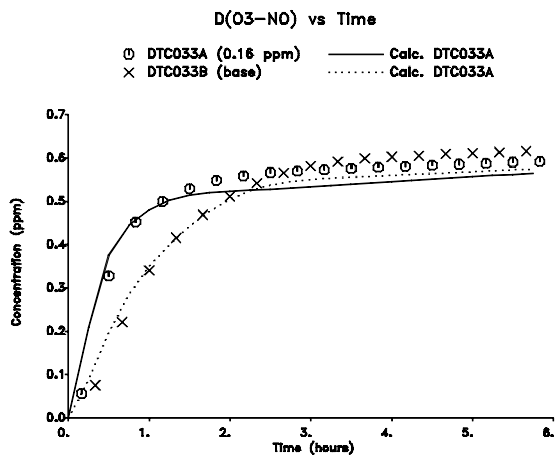
Figure 44. Plots of selected results of the low NO_x lumped molecule surrogate reactivity experiment for **trans-2-Butene**

99
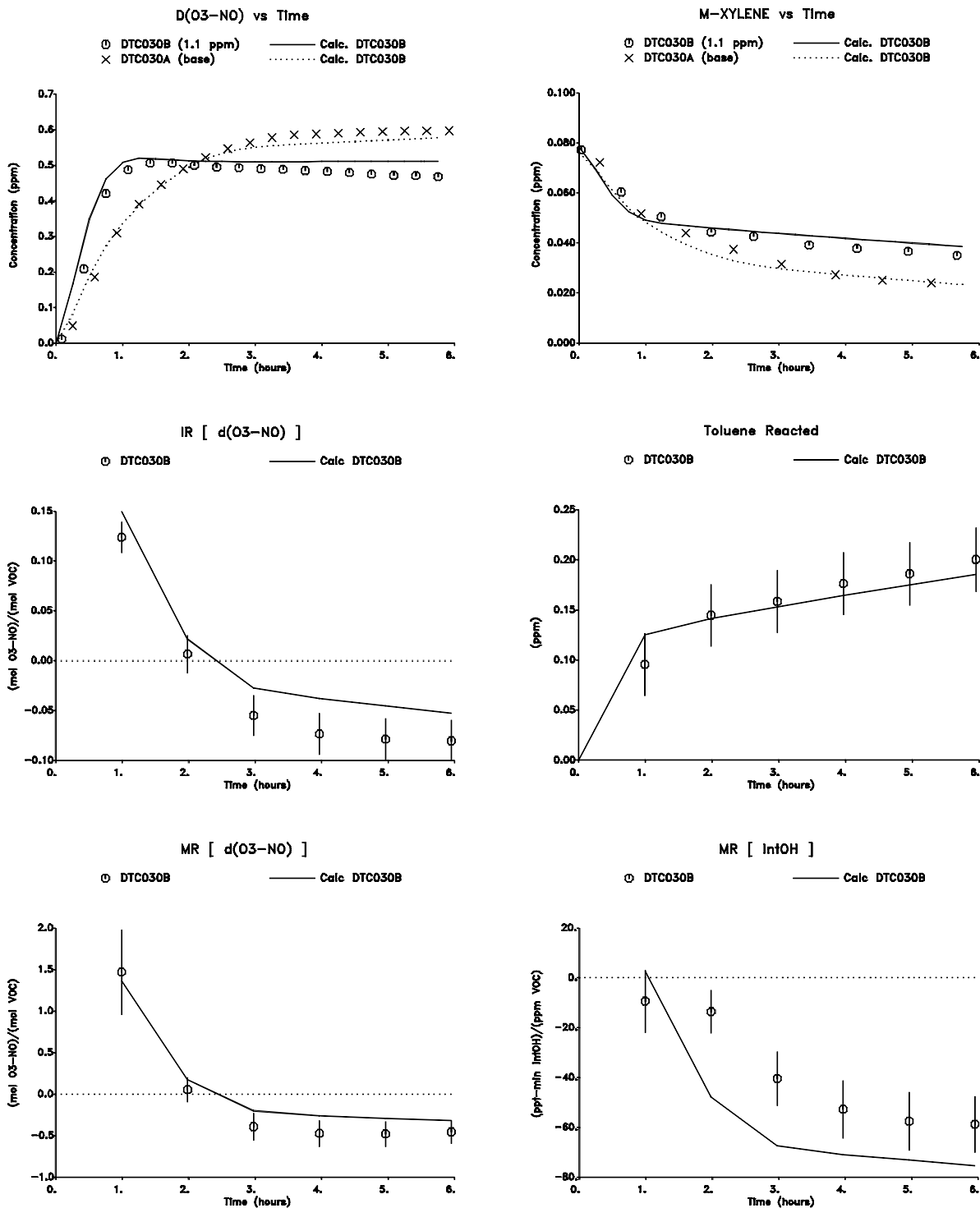
Figure 45. Plots of selected results of the low NO_x lumped molecule surrogate reactivity experiment for **toluene**
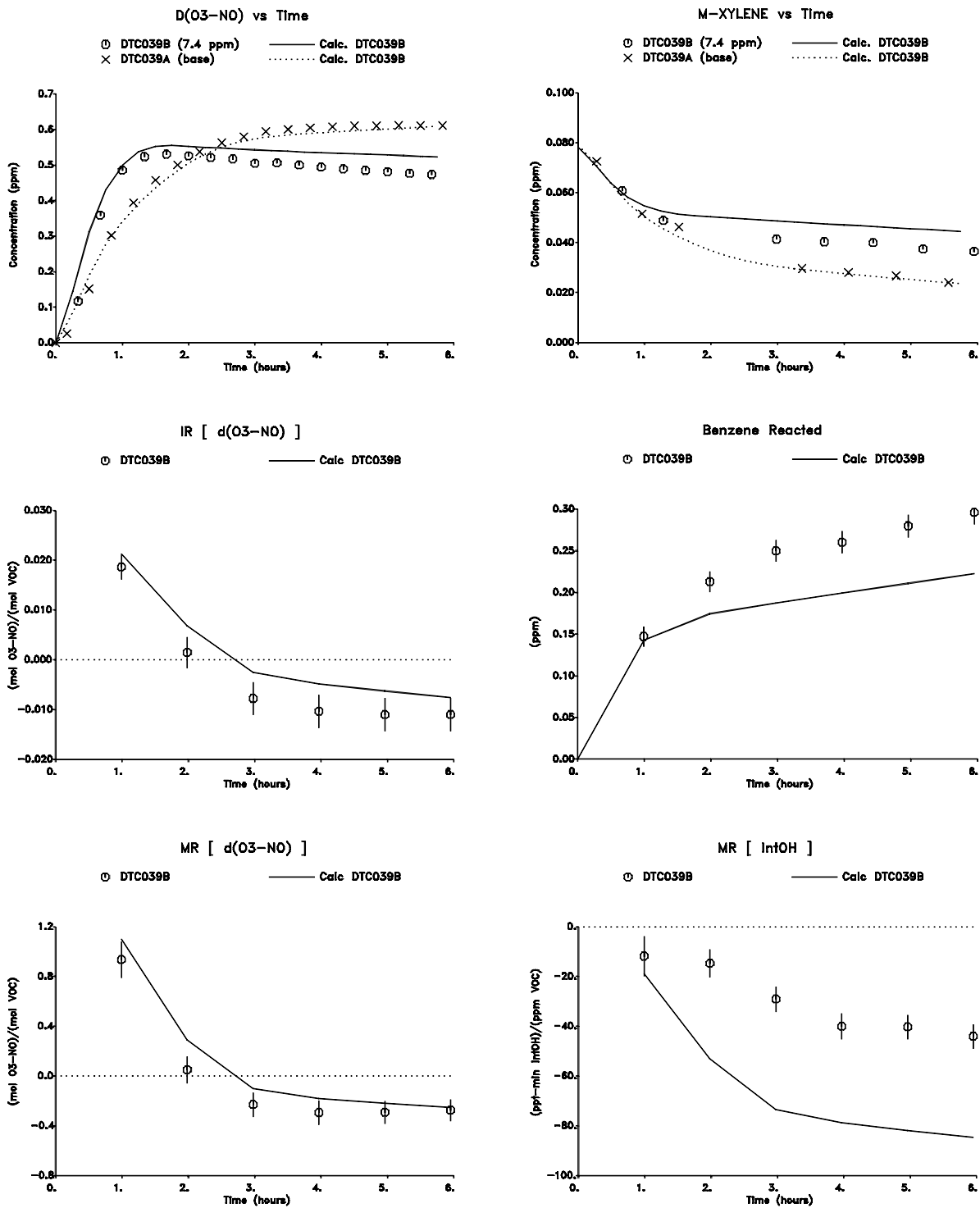
Figure 46. Plots of selected results of the low NO_x lumped molecule surrogate reactivity experiment for **benzene**
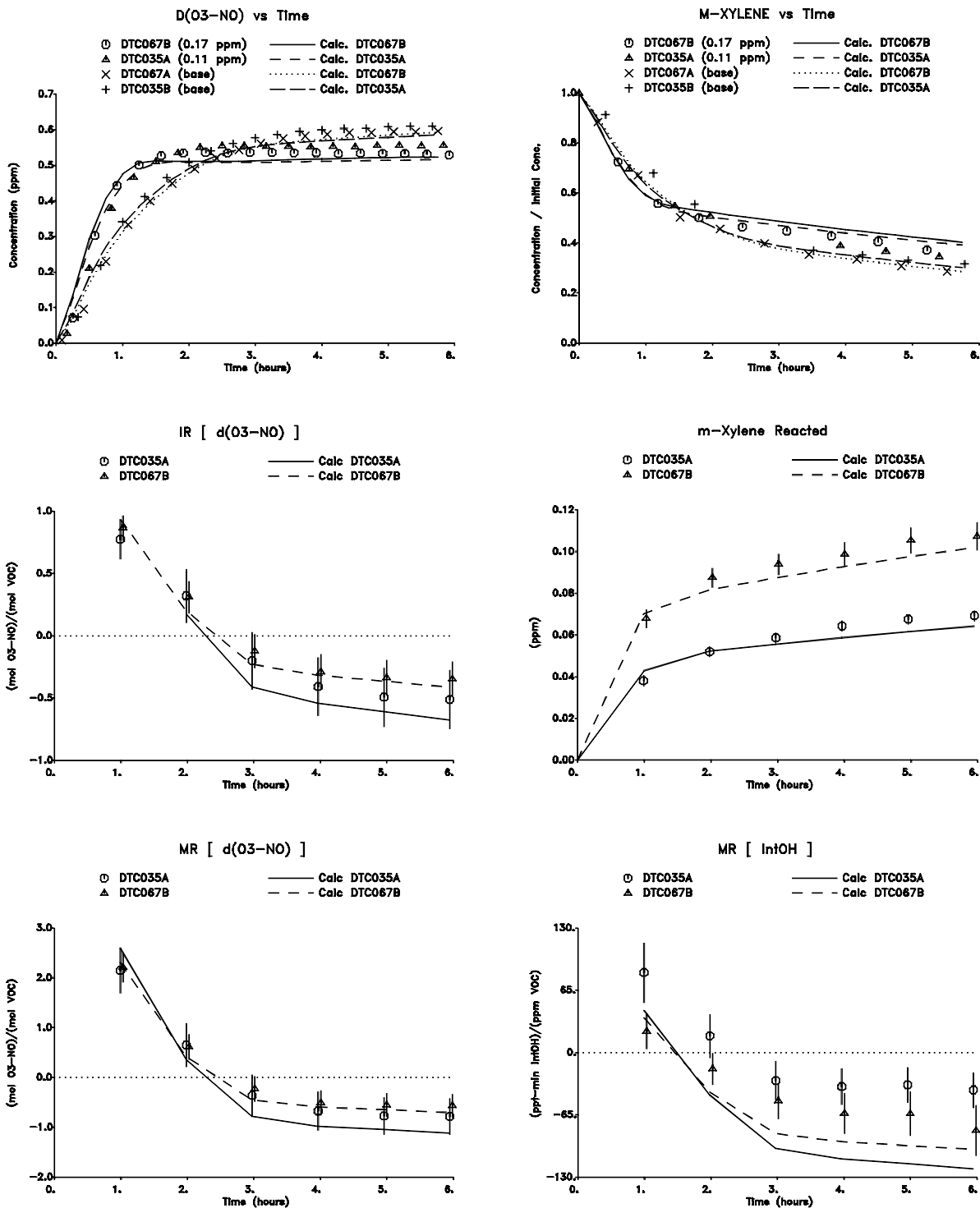
Figure 47. Plots of selected results of the low NO_x lumped molecule surrogate reactivity experiments for **m-xylene**

D(O3-NO) vs Time

⊙ DTC036A (0.25 ppm) —— Calc. DTC036A
✕ DTC036B (base) ······ Calc. DTC036A

M-XYLENE vs Time

⊙ DTC036A (0.25 ppm) —— Calc. DTC036A
✕ DTC036B (base) ······ Calc. DTC036A

IR [d(O3-NO)]

⊙ DTC036A —— Calc DTC036A

IR [IntOH]

⊙ DTC036A —— Calc DTC036A
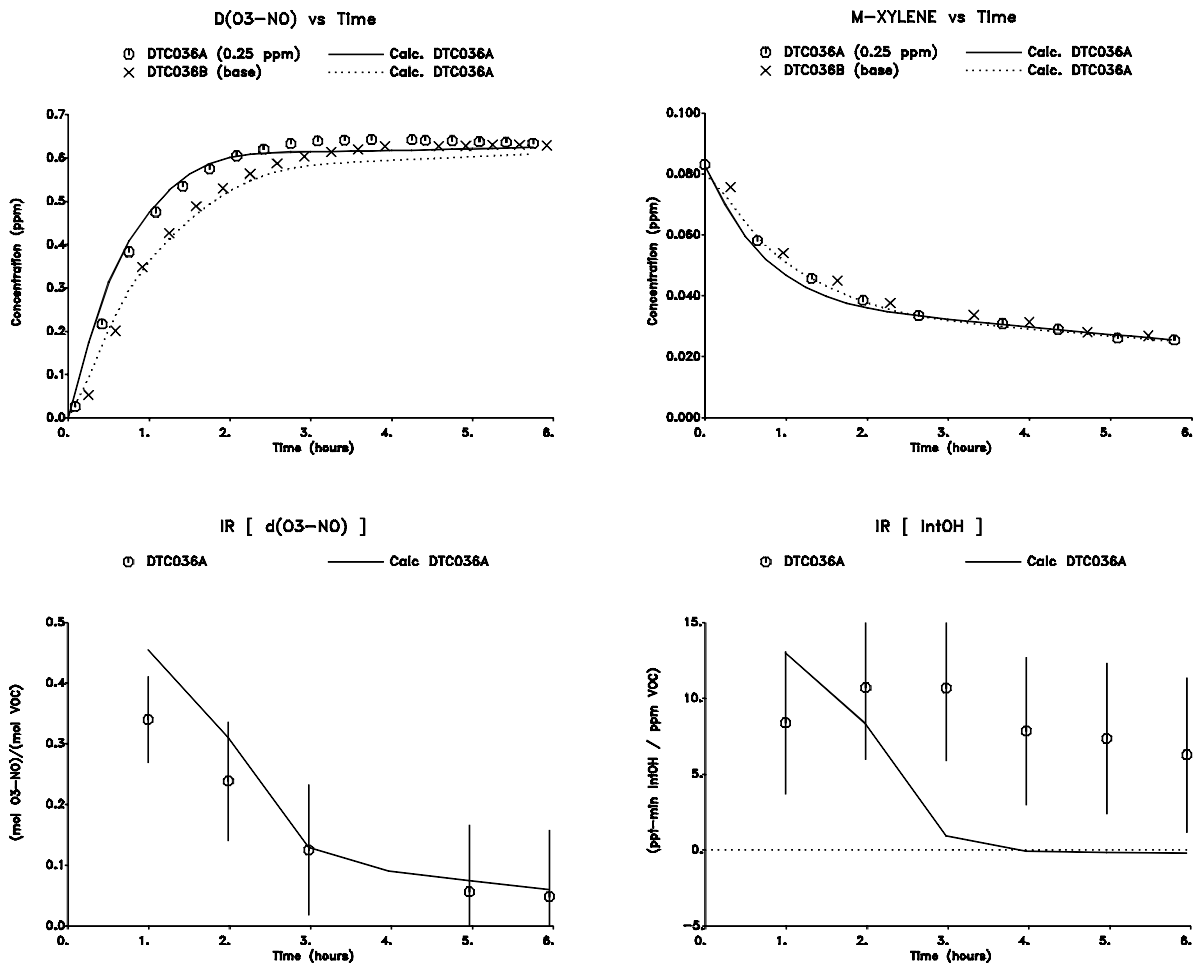
Figure 48. Plots of selected results of the low NO_x lumped molecule surrogate reactivity experiment for **formaldehyde**

103

D(O3-NO) vs Time

- DTC066B (1.6 ppm) — Calc. DTC066B
- × DTC066A (base) ⋯⋯ Calc. DTC066B

M-XYLENE vs Time

- DTC066B (1.6 ppm) — Calc. DTC066B
- × DTC066A (base) ⋯⋯ Calc. DTC066B

IR [d(O3-NO)]

- DTC066B — Calc DTC066B

Acetaldehyde Reacted

- DTC066B — Calc DTC066B

MR [d(O3-NO)]

- DTC066B — Calc DTC066B

IR [IntOH]

- DTC066B — Calc DTC066B
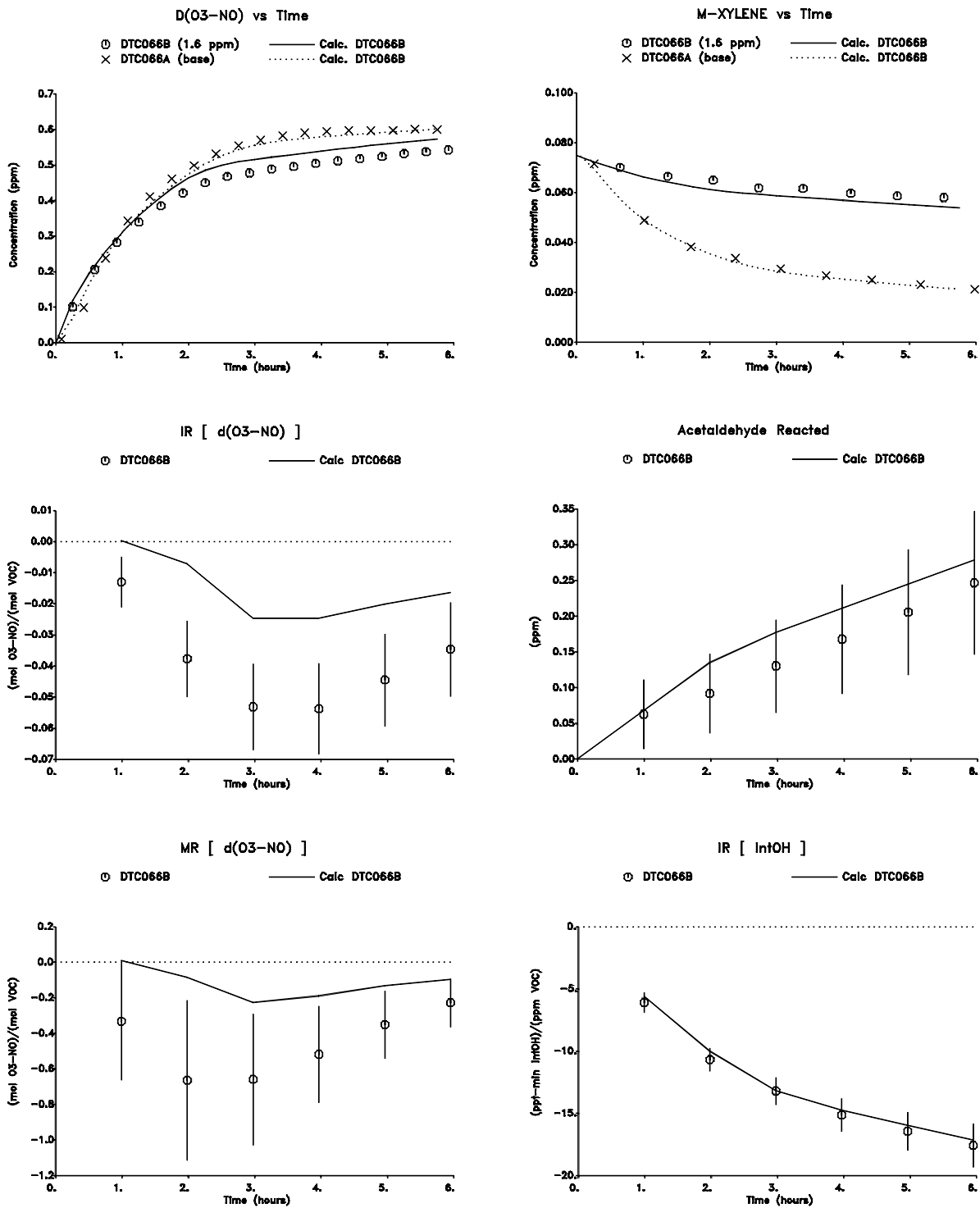
Figure 49. Plots of selected results of the low NO_x lumped molecule surrogate reactivity experiment for **acetaldehyde**

104

V. MODEL SIMULATIONS

A major objective of this study is to provide data to test the ability of chemical mechanisms used in airshed models to correctly predict VOC reactivities, and in particular how VOC reactivities vary with differing base ROG and NO_x. Although a complete mechanism evaluation and update using these data is beyond the scope of the present report, model calculations were carried out to determine the extent to which the predictions of an updated version of the detailed SAPRC mechanism (Carter, 1990, Carter et al. 1993a; Carter, 1993, Carter et. al., 1993b) are consistent with these new data. The mechanism and approach used to simulate the chamber experiments, and the results obtained, are summarized in this section. The implications of these results are discussed in the Discussion and Conclusions sections.

A.   Chemical Mechanism
The chemical mechanism employed in the chamber model simulations given in this report has been documented in the report on our study of the reactivity of acetone (Carter et al., 1993b). The starting point for this mechanism was the "SAPRC-91" mechanism documented in the report on Phase I of this program (Carter et al., 1993b), which was further updated and modified as discussed below. The SAPRC-91 mechanism is an updated version of the "SAPRC-90" mechanism which was used to calculate the MIR reactivity scale used in the CARB regulation (Carter, 1993, 1994; 1991). The differences between the current mechanism, which will be referred to as the "SAPRC-93" mechanism in the subsequent discussion, and the earlier versions of the SAPRC detailed mechanisms are summarized below. Note that some of the changes are not relevant to the specific simulations in this report, but are included in the discussion below for completeness.

(1) The updates to the formaldehyde absorption cross-sections and the kinetics of PAN formation incorporated in the SAPRC-91 mechanism were also incorporated in this mechanism. The changes in PAN kinetics cause the model to predict somewhat higher ozone formation rates than the SAPRC-90 mechanism.

(2) The SAPRC mechanisms use model species whose photolysis rates are adjusted to fit aromatic-NO_x-air chamber experiments to represent the unknown photoreactive aromatic fragmentation products (Carter, 1990). In the SAPRC-91 and the current mechanisms, the action spectra (absorption coefficients x quantum yields) for these products were assumed to be proportional to the absorption cross section for acrolein (Gardner et al., 1987), rather than using the somewhat arbitrary action spectrum in the SAPRC-90 mechanism. The yields of these products were reoptimized based on the simulations of the available chamber data using the updated mechanism. In the SAPRC-91 mechanism, different optimizations were used for m-xylene, depending on which experiments were being simulated (Carter et al., 1993a). In this work, the same m-xylene was used in all simulations, with the parameters optimized to fit m-xylene - NO_x - air

experiments. This resulted in a mechanism which somewhat underpredicted the results of many of the "Set 3" Phase I mini-surrogate experiments, though it performed much better than did the "unadjusted SAPRC-91" mechanism used in the Phase I report, and it performed reasonably well in simulating the base case experiments in this study (see below). The NO_x data for all the relevant aromatic experiments were corrected as discussed by Carter et al. (1995b) prior to reoptimizing the aromatic product yield parameters.

(3) The mechanisms for the reactions of ozone with alkenes were modified to be consistent with the data of Atkinson and Aschmann (1993), who observed much higher yields of OH radicals than predicted by the SAPRC-90 and SAPRC-91 mechanisms. To account for these data, it was assumed that (1) the formation of OH radicals dominates over other radical-forming fragmentation processes, and (2) in the reactions of unsymmetrical alkenes, the more substituted Criegee biradical, which forms higher OH yields, are formed in relatively higher yields than the less substituted biradicals. The modified ozone reactions for the alkenes discussed in this paper are:

    Ethene + O3 -→ HCHO + (HCHO2)
    Propene + O3 -→ 0.6 HCHO + 0.4 CCHO + 0.4 (HCHO2) + 0.6 (CCHO2)
    trans-2-Butene + O3 -→ CCHO + (CCHO2)
    Isobutene + O3 -→ 0.82 HCHO + 0.18 ACET + 0.18 (HCHO2) + 0.82 (C(C)CO2)
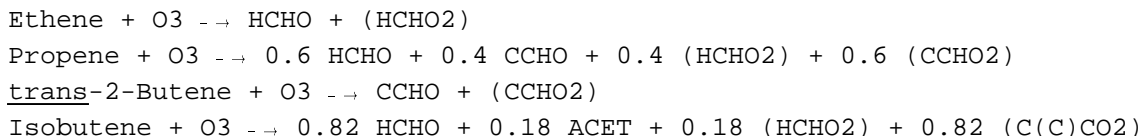
where CCHO and ACET represent acetaldehyde and acetone, and (HCHO2), etc., represent the excited Criegee biradicals, which are represented as reacting as follows:

(HCHO2) $\xrightarrow{fast}$ 0.12 CO + 0.12 HO. + 0.12 HO2. + 0.88 (unreactive carbon)

(CCHO2) $\xrightarrow{fast}$ 0.3 HCHO + 0.3 CO + 0.6 HO. + 0.3 {CCO-O2.+ RCO3.} + 0.3 {RO2-R.+ RO2.} + 0.9 (unreactive carbon)

(C(C)CO2) $\xrightarrow{fast}$ HCHO + HO. + {R2O2.+ RO2.} + {CCO-O2.+ RCO3.}
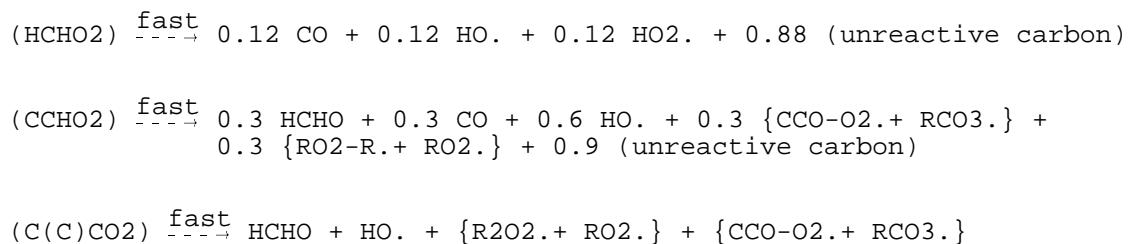
[See Carter (1990) for a description of the model species and the methods used to represent peroxy radical reactions.] This is clearly an oversimplification of this complex system (e.g., see Atkinson, 1990, 1994), but is intended to account for the observed OH radical yields and represent the major features affecting these compounds' reactivities. Note that this new mechanism gives substantially higher radical yields in the ozone + alkene systems than the SAPRC-90 mechanism, particularly for internal alkenes.

(4) The reaction of NO with the peroxy radical formed in the reaction of OH radicals with isobutene was assumed to form the corresponding hydroxyalkyl nitrate 10% of the time. This assumption resulted in significant improvements

to the fit of model simulations to ozone and PAN yields in isobutene - NO$_x$ - air chamber experiments. Without this assumption, the model with the OH yields indicated by the O$_3$ + isobutene data of Atkinson and Aschmann (1993) significantly overpredicts O$_3$ formation rates. If lower radical yields in the O$_3$ + isobutene reaction are assumed, the model significantly underpredicts PAN (unpublished results from this laboratory).

(5) The representation of iso-octane was modified to improve the model simulations of its reactivity (Carter et al., 1993a).

(6) Several changes were made to the mechanism for acetone. These are documented elsewhere (Carter et al., 1993b.) Note that the mechanism used in this work employed the acetone quantum yields based on the corrected data of Meyrahn et al. (1986), and not the values adjusted to fit our recent chamber experiments (Carter et al., 1993b). Although this is a potential source of uncertainty, it only affects predictions of acetone's reactivity, and has no substantial effect on any of the simulations discussed in this report.

A listing of the SAPRC-93 mechanism is given by Carter et al. (1993b). Further updates to this mechanism are planned, and the process of evaluating it against the full data base of chamber experiments (Carter and Lurmann, 1991; Carter et al., 1995b) is underway. However, it was evaluated in model simulations of the results of the extensive set of Phase I reactivity experiments (Carter et al, 1993c), and was found to perform somewhat better than the SAPRC-90 and SAPRC-91 mechanisms in simulating these data.

B.   Chamber Modeling Procedures
The testing of a chemical mechanism against environmental chamber results requires including in the model appropriate representations for the characteristics of the light source, run conditions and chamber-dependent effects such as wall reactions and chamber radical sources. The methods used to represent them in this study are based on those discussed in detail by Carter and Lurmann (1991), modified as discussed by Carter et al. (1995b), and adapted for these specific sets of experiments as indicated below. Where possible, the parameters were derived based on analysis of results of characterization experiments carried out in conjunction with these runs. The specific chamber-dependent parameters used in chamber model simulations for this study, and their derivations are as follows:

1.   Photolysis Rates
The photolysis rates when simulating indoor chamber experiments are calculated given the NO$_2$ photolysis rate and the relative spectral distribution assigned for the run. The NO$_2$ photolysis rate used in modeling the ETC runs in this study was 0.351 min^{-1}. This was derived using the fits to the ETC actinometry data discussed by Carter et al., 1993a, with the fits recalculated to incorporate the newer experiments carried out in conjunction with the runs for

this program, and using NO_2 photolysis rates derived using slightly modified effective quantum yield parameter as discussed elsewhere (Carter et al., 1995b). The results of the newer ETC experiments were entirely within the range predicted based on the earlier runs. The NO_2 photolysis rate used when modeling the DTC runs was based on the average of the results of all the actinometry experiments carried out in this chamber after the reaction bag was installed, which was 0.388 ± 0.011 min^{-1}. (No decay of NO_2 photolysis rate with time was observed for this chamber, presumably because the blacklights were turned on and "burned in" for several weeks before being used.) The detailed data base and derivation of the NO_2 photolysis rates of experiments in these and other chambers is given in a separate document (Carter et al., 1995b).

The quantum yields used when simulating the DTC and ETC experiments were based on the composite spectrum which we now recommend using when modeling SAPRC blacklight chamber runs (Carter et al. 1995b). It is somewhat different than that we employed previously in our simulations of chamber experiments (Carter and Lurmann, 1991; Carter et al., 1993a-c), being significantly better in representing the many mercury emission lines. This change was found to have a non-negligible effect on the calculation of certain photolysis rates, though the effect of this change has not yet been systematically evaluated.

2. Run Conditions

Temperature: The average temperatures for these experiments are given on Tables 7 and 11. The temperature used when modeling the experiments was based on fitting the temperature data to a series of line segments (usually two — one to represent the relatively rapid increase in temperature during the first ~15 minutes of the run, the other to represent any small trend in temperature later), as recommended when modeling SAPRC chamber runs (Carter et al., 1995b). The temperature in the model simulation changed linearly between the times defining the end points of these segments. Note that this differs slightly from our previous procedure of using a constant temperature (based on the average during the run) when modeling indoor chamber runs.

Humidity: Unhumidified air was used in these experiments because it minimizes chamber effects and improves reproducibility. Measurements made previously indicate the unhumidified output of the SAPRC pure air system typically has humidities of approximately 5%. This corresponds to approximately 5000 ppm of H_2O, which was used in the model simulations.

Dilution: The dilution rates used in simulating these experiments were the same as those used when analyzing the reactivity data, which were derived as discussed above. For non-reactivity experiments, the dilution rates were derived in an analogous manner. The values used for the individual experiments is given with documentation for the SAPRC chamber data base (Carter et al., 1995b).

3. Chamber Effects Parameters

Initial Nitrous Acid: Nitrous acid (HONO) can sometimes be introduced into the chamber during NO_x injection (Carter and Lurmann, 1990, 1991), and if present can affect rates of NO oxidation at the beginning of the run because of its rapid photolysis to form OH radicals. There was evidence for HONO contamination during our initial Phase I experiments, but this was apparently eliminated by injecting NO_x using vacuum techniques (Carter et al., 1993a). Since these vacuum methods were used for the NO_x injections in all the runs in this study, we assume that initial HONO is negligible in the simulations of these runs. Results of comparisons of model simulations with data from control and characterization runs are consistent with this assumption.

Continuous Chamber Radical Source: As discussed previously (Carter et al., 1982; Carter and Lurmann, 1990, 1991) there is a continuous chamber-dependent radical source which must be accounted for in model simulations of environmental chamber experiments. The magnitude of this radical source is extremely important in affecting simulations of alkane-NO_x-air experiments and other low reactivity runs, though it is less important — though not negligible — when simulating surrogate-NO_x-air runs such as these reactivity experiments (Carter and Lurmann, 1991). This can be determined by model simulations of radical tracer-NO_x-air experiments (Carter et al., 1982), or alkane-NO_x-air experiments. The radical input rate used in the model simulations of the ETC runs for this program was 0.04 ppb x k_1, based on model simulations of the tracer-NOx-air experiments ETC-380 and 472. This is slightly higher than the radical input rates used to simulate the Phase I ETC experiments, though is not inconsistent with results of the tracer-NO_x and n-butane-NO_x runs carried out in conjunction with those runs. The radical input used when modeling the DTC runs was 0.05 ppb x k_1, based on simulations of tracer-NO_x-air run DTC058 and n-butane-NO_x-air run DTC059. Note that this is not significantly different than that used when modeling the ETC runs.

NO_x Offgasing Rate A light-dependent offgasing of NO_x also occurs in environmental chamber experiments. This can affect predictions of maximum O_3 yields in low NO_x experiments. The rate of this offgasing can be derived by model simulations of O_3 formation in pure air irradiations and on O_3 and PAN formation in acetaldehyde-air irradiations. The NO_x offgasing rates used in the simulations of the ETC and DTC runs for this program were k_1 x 0.4 ppb and k_1 x 0.3 ppb, respectively. These are based on based on simulations of ozone formation in the acetaldehyde-air run ETC382 and in the pure air runs ETC458, ETC485 and DTC049. A slightly lower NO_x offgasing rate might be expected in the DTC than the ETC because of the larger chamber volume, though the difference is probably well within the uncertainty of the determination. Lower NO_x offgasing rates were assumed in the simulations of the Phase I experiments, but this was based on modeling a pure air irradiation in a relatively new chamber.

NO Conversion Due to Background VOCs. The effect of background organics is represented by a conversion of HO to HO_2 at a rate adjusted to fit pure air experiments (Carter and Lurmann, 1990, 1991). These simulations used the same rate as derived for the SAPRC ITC, or 250 min^{-1}. This fits model simulations of the ETC and DTC pure air runs reasonably well. The simulations of reactivity experiments are insensitive to this parameter.

Ozone Decay Rate: The O_3 dark decay rates measured in the ETC reaction bag used in this program were 2.7 x 10^{-4} min^{-1} when the bag was relatively new (ETC374) and was 1.21 and 1.23 x 10^{-4} min^{-1} in two experiments in the well conditioned bag. The average of the latter two values was used when modeling the ETC runs. The O_3 dark decay was measured in the DTC only when the reaction bags were new, and the result was 2.5 x 10^{-4} min^{-1} for both sides, making it very similar to the O_3 decay in the ETC with the new reaction bag. Based on the results with the ETC, one would expect lower O_3 decays when the bags were more conditioned. For modeling the DTC runs, where O_3 decay measurements were only made when the chamber was new, we assumed an O_3 decay rate of 1.5 x 10^{-4} min^{-1}, which is similar to the value used for the ETC and is the recommended default for modeling SAPRC ITC runs (Carter et al., 1995b).

N_2O_5 Hydrolysis: The rate of the heterogeneous hydrolysis of N_2O_5 used when modeling these experiments was as recommended by Carter et al. (1995b) for modeling SAPRC teflon chamber runs, and is as follows:

Rate $(N_2O_5+H_2O)$ = 2.8 x10^{-3} + $(1.5 \times 10^{-6} - k_g)$ [H_2O (ppm)] ppm min^{-1},

where k_g is the rate constant used in the gas-phase mechanism for the $N_2O_5+H_2O$ reaction. This is based on the N_2O_5 decay rate measurements in the ETC reported by Tuazon et al. (1983). Although we previously estimated there rate constants were lower in the larger Teflon bag chambers (Carter and Lurmann, 1990, 1991), we now consider it more reasonable to use the same rate constants for all such This parameter affects predictions of O_3 yields in runs which are NO_x-limited.

4.   Modeling Experimental Incremental Reactivities

DTC Experiments. The model simulations of incremental reactivities measured in the DTC experiments consisted simply of conducting simulations of the added VOC (test) experiment and the simultaneous base case experiment, and then incremental and mechanistic reactivities from the calculated data in the same way as derived from the experimental data. Thus, each model simulation of incremental reactivity in the DTC took into account the particular conditions of each divided chamber experiment, and did not require any assumptions concerning consistency of conditions from experiment to experiment. This is applicable to the simulations of all the lumped surrogate experiments and the ethene surrogate experiment with n-hexane.

ETC Experiments. The approach used when modeling the reactivities in the ETC runs was to conduct simulations for the conditions of each test compound experiment, and then repeat the simulations with the same conditions, but with the test compound removed. The latter simulation was then used to represent the base case. Note that this is somewhat different than the approach used when modeling the Phase I ETC reactivity experiments (Carter et al., 1993a). In that study, the base case simulation for all experiments consisted of simulating an "averaged conditions" base case experiment, and then simulating individual reactivity experiments by simulating the averaged conditions base case with the appropriate amount of test compound added. The approach used in this work has the advantage that the specific conditions of each individual experiment are taken into account. However, the "averaged conditions" approach was used when preparing the calculated data on the plots of incremental reactivity as a function of VOC added.

C.   Model Simulation Results

1.   Base Case Experiments

Phase I Mini-Surrogate Runs. Before discussing the simulations of the mini-surrogate experiments in this work, it is useful to discuss the current status of the model in simulating the standard mini-surrogate run used in the Phase I reactivity study (Carter et al., 1993a). In the report on that program, we were unable to simulate all the three sets of base case experiments using the same version of the mechanism, and had to adjust the m-xylene mechanism to get acceptable fits to the "Set 3" mini-surrogate runs. To see if this is still the case, we used the current version of the mechanism to simulate the representative Phase I base case experiments which were used to illustrate model performance in the Phase I report (figures 7-9 in Carter et al., 1993a). The results are shown on Figure 50, which shows experimental and calculated concentration-time profiles for ozone, NO, NO2 (or NO_y-NO) and m-xylene. Figure 50 also gives a plot of the relative errors in the model calculation[1] against the average temperature in the Set 3 runs. It can be seen that the model now performs somewhat better in simulating these experiments. Although it still underpredicts the rate of O_3 formation in the many of the Set 3 run, the discrepancy is much less than was the case previously. The discrepancy for the Set 3 runs can also be seen to be dependent on the average temperature, with good fits being obtained for runs carried out at ~300°K. (The temperature effects on model performance are discussed in more detail elsewhere [Carter et al., 1995a].)

The reason for the improved performance of the mechanism in simulating the Phase I can be attributed in part to corrections to the SAPRC chamber data base carried out under EPA and CARB funding (Carter et al., 1995b), in part to a re-evaluation of chamber effects parameters for this chamber (Carter et al., 1995a), and in part to the updates to the chemical mechanism. However, none of these runs were used in optimizing the parameters of the current version of the

---

[1](model - experiment) / (average of model and experiment)
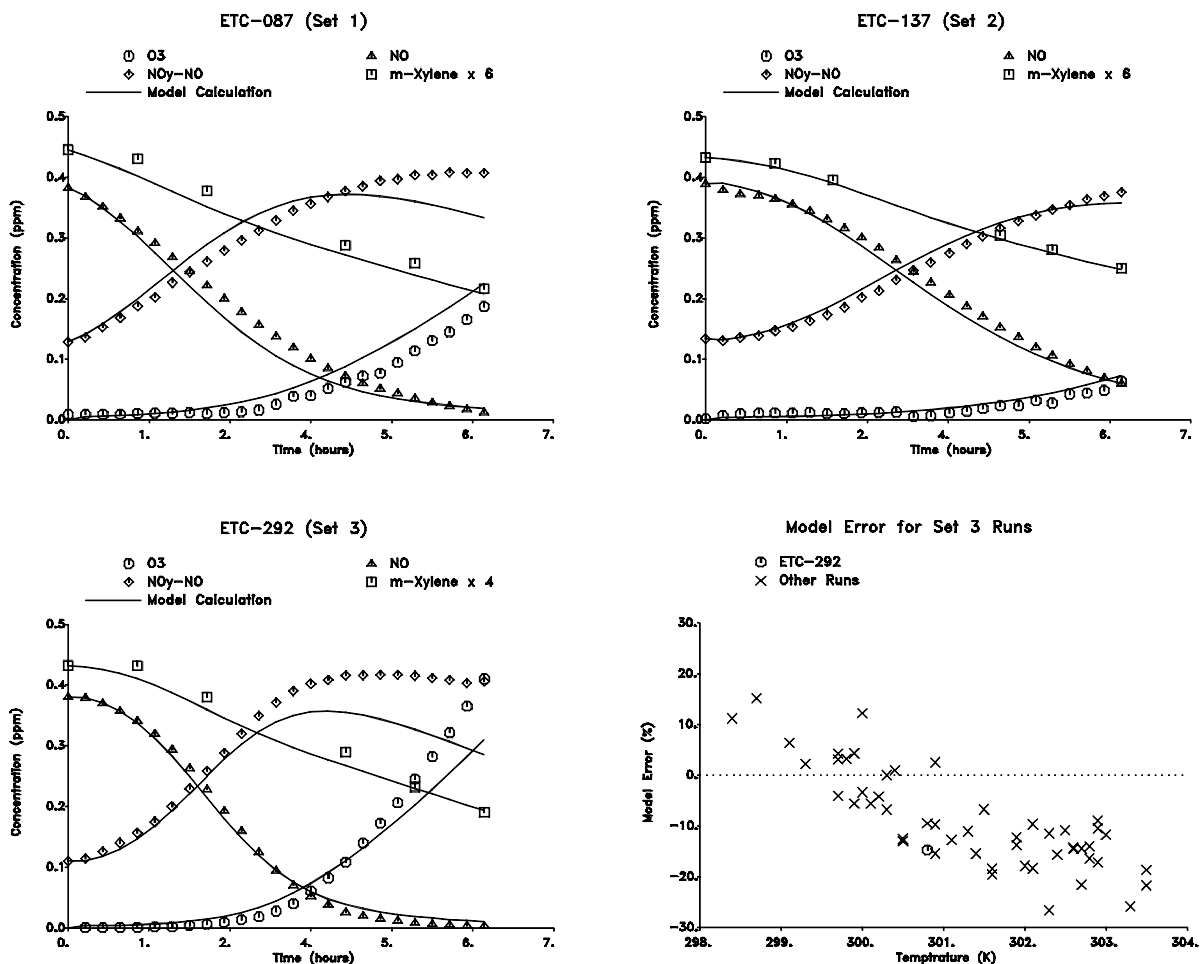
Figure 50. Experimental and calculated concentration-time profiles for selected species in selected Phase I base-case mini-surrogate experiments, and plots of relative errors in model calculations of the Set 3 runs against average temperature.

m-xylene mechanism, nor was there a change in the formulation of the m-xylene mechanism or the way it is parameterized. Non-negligible corrections were made to some of the NO_x data in several of the runs used to derive the aromatic mechanistic parameters, and the spectral distribution used to calculate photolysis rates when modeling runs with blacklight light sources was refined. The modifications to the chamber effects parameters used when simulating the ETC runs included increasing the magnitude of the chamber radical source parameter for the ETC for the period of time when most of the Set 3 runs were conducted. This latter change, which was based on modeling n-butane-NO_x and tracer-NO_x-air runs, is probably the major contributor to the improvement.

Ethene Surrogate Runs. Examples of results of model simulations of the base case ethene surrogate runs are shown on Figure 15, above, and Figure 51
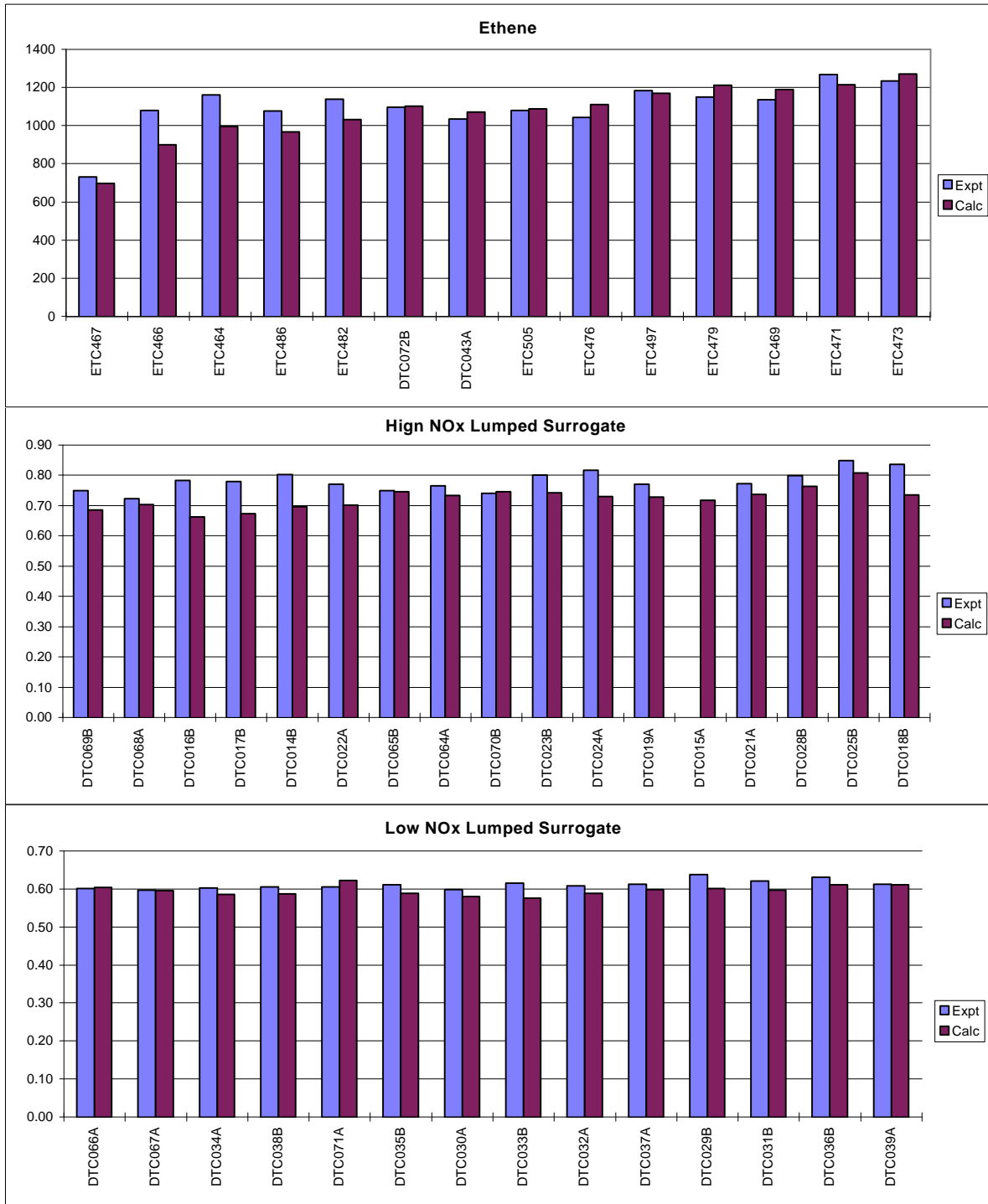
Figure 51. Comparisons of experimental and calculated 6-hour
d(O3-NO) for the base case experiments. Units are ppm.

shows a comparison of the experimental and calculated final d(O$_3$-NO) for all the base case runs. The runs on Figure 51 are sorted by ascending initial base ROG concentration. It can be seen that reasonably good fits are obtained, but that there is some scatter in the fits to the ethene runs.

The scatter in model fits to the ethene runs appears to be due more to variation in the calculated d(O$_3$-NO) than in the experimental data. A possible explanation for this may be errors in the measured values of ethene, which are used to determine the initial concentrations of the simulations. In particular, the runs with the underprediction of greater than 10% all have initial ethene concentrations which are less than the average, and much better fits of model simulations to the results of these experiments are used if initial ethene levels more typical of the other runs are used. However, there are no apparent problems with the ethene calibrations or data with those runs.

The regression analysis of the experimental ethene data suggest a slight temperature dependence in the ethene data. As discussed elsewhere (Carter et al., 1995a), this is not predicted by the model, even after taking into account possible temperature-dependent chamber effects. However, the effect of other variations in run conditions, particularly initial ethene, appears to be more important in affecting the fits than variations in temperature, since there is no clear correlation between average run temperature and model prediction error.

Lumped Surrogate Runs. Examples of model simulations of the high and low NO$_x$ base case lumped surrogate runs are shown on Figures 24 and 25, above, and Figure 51 shows a comparison of the experimental and calculated final d(O$_3$-NO) for all these runs. It can be seen that, with the exception of the formaldehyde data, the model performs reasonably well in simulating these runs. The model slightly underpredicts the O$_3$ formation rate in the high NO$_x$ lumped surrogate runs, in a manner similar to the underprediction of O$_3$ formation in most of the Phase I mini-surrogate runs (see Figure 50). The discrepancy is not sufficient to warrant adjusting the mechanisms for the purpose of simulating incremental reactivity.

We have no explanation for the poor performance of the model in simulating the formaldehyde profiles in these runs. The mechanisms for some of the base ROG surrogate components may not be including sufficient formaldehyde sources. However, another explanation is that there is an interference in the formaldehyde analysis with some other product(s) formed in this system. This will be investigated in the subsequent program. This is not considered to be a major concern for this program, where the focus is effects of VOCs on ozone and OH radicals. We believe the initial formaldehyde measurements are correct, because they are consistent with the amounts of formaldehyde injected, which are measured with some accuracy using vacuum methods with capacitance manometers and bulbs of known volume.

114

2. Ethene Surrogate Reactivity Experiments

Figures 15-23, above, show the results of the model simulations of the $d(O_3-NO)$ data and the various measures of reactivity in the ethene reactivity experiments with the various test VOCs. Figures 52-54 show plots of the calculated vs. experimental 6-hour $d(O_3-NO)$, IntOH, and estimated direct mechanistic reactivities for the various experiments, where the performance of the model for the ethene surrogate experiments can be compared with that for the other surrogates. (Note that the reactivity data on Figures 52-54 are given on a per carbon basis, while all such data given on previous figures and tables are on a per molecule basis.) In general, the performance of the model in simulating reactivities in the ethene surrogate runs was variable. Good fits for essentially all reactivity measures were obtained with CO, ethane and m-xylene. Fair fits, which can probably be considered to be within experimental and/or model characterization variability, were obtained for n-hexane, propene, and trans-2-butene. Poor fits were obtained for n-octane, formaldehyde, and, to a lesser extent, n-butane.

The model was found to significantly overpredict the incremental reactivity of formaldehyde in the run with the lowest amount of added formaldehyde, and during the initial periods of all the runs. This is consistent with the underprediction of formaldehyde reactivity observed when modeling the Phase I mini-surrogate runs (Carter et al. 1993a). The model was also found to significantly underpredict, by approximately a factor of two, of the inhibition of $d(O_3-NO)$ caused by n-octane. A similar result, though to a much lesser extent, is seen in the model simulations of the added n-butane and n-hexane runs. The quality of the IntOH data in the added alkane ethene surrogate runs is not sufficient to clearly indicate whether the source of the discrepancy is the model simulation of the effect of these alkanes on radical levels, or their direct reactivities. These cases of poor model performance will be discussed further below.

3. High NO_x Lumped Surrogate Reactivity Experiments

Figures 29-38, above, show the results of the model simulations of the data from the high NO_x lumped surrogate reactivity runs. In general, remarkably good performance in the model simulations of the reactivity data was observed, considerably better in general than the simulations of the reactivities in the ethene surrogate runs. Even the reactivities of n-octane and formalde-hyde, which were poorly simulated by the model in the ethene surrogate, were well fit with the more complex lumped surrogate runs. This is despite the greater experimental precision observed in these runs, and the higher quality IntOH data, which gave a more precise test of the mechanism.

The only discrepancies between model and experiment which might be outside the range of experimental or run characterization uncertainty are as follows.
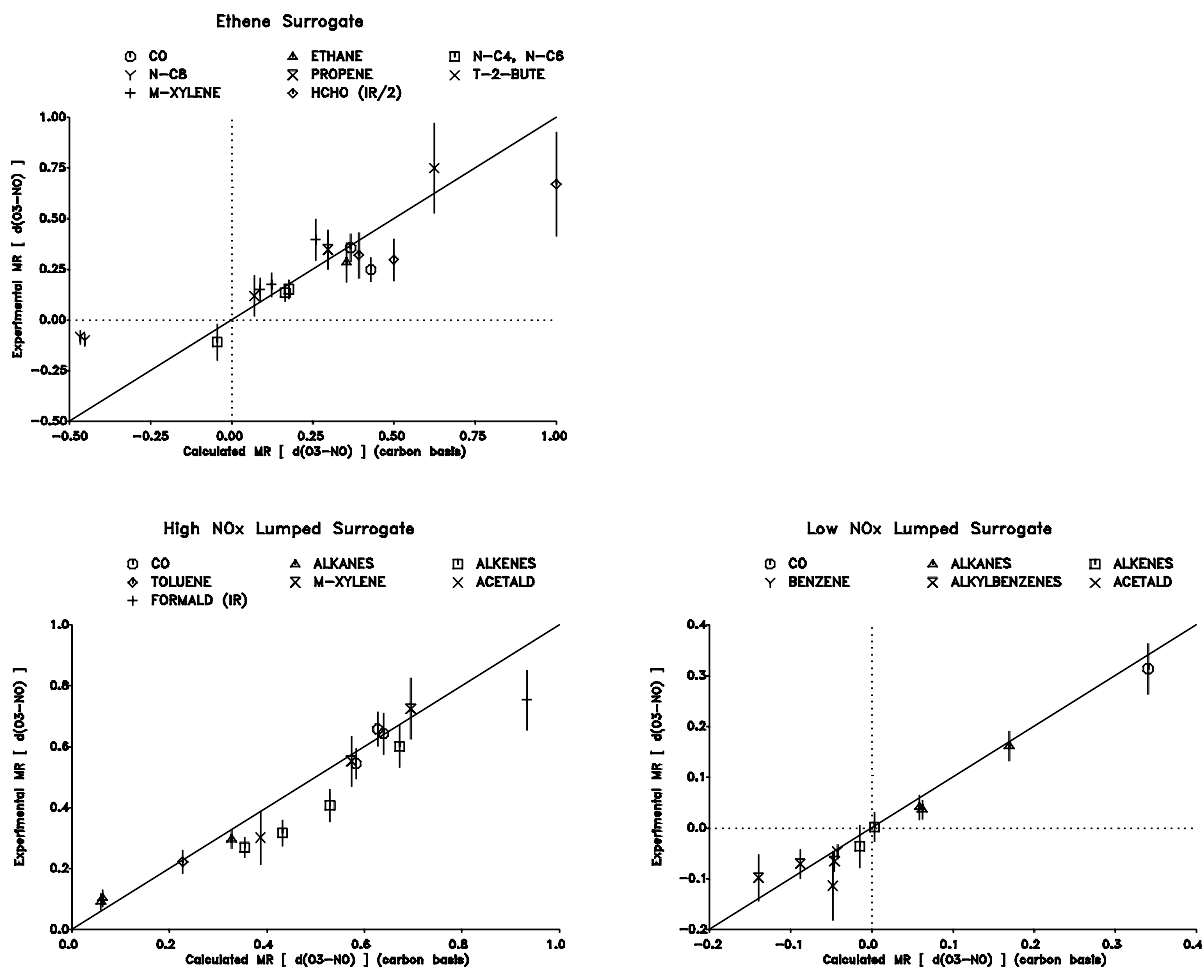
Figure 52. Plots of experimental vs calculated 6-hour $d(O_3\text{-}NO)$ mechanistic reactivities for the various types of reactivity runs. Note that the reactivities are given on a per-carbon basis.

The $d(O_3\text{-}NO)$ and IntOH reactivities of CO, n-butane (for the initial part of the experiment) and toluene are slightly underpredicted. (2) The IntOH reactivity of n-butane is slightly underpredicted. The model somewhat overpredicts the rates of O_3 formation at the end of the added propene and trans-2-butene runs, causing an overprediction of $d(O_3\text{-}NO)$ reactivities at the end of the runs. However, in all cases, the discrepancies are small and may not necessarily indicate problems with the mechanism.

4. Low NO$_x$ Lumped Surrogate Reactivity Experiments

Figures 39-49, above, show the results of the model simulations of the low NO$_x$ lumped surrogate reactivity runs. In general, the performance of the model was almost as good in simulating these runs as in simulating the high NO$_x$ lumped surrogate runs, though there were some cases where perhaps more

Ethene Surrogate

☉ CO	▲ ETHANE	⊡ N−C4, N−C6
Y N−C8	✕ PROPENE	✕ T−2−BUTE
+ M−XYLENE	◇ HCHO (IR)	

Experimental MR [IntOH] vs *Calculated MR [IntOH] (ppt−min/ppmC)*

High NOx Lumped Surrogate

| ☉ CO | ▲ ALKANES | ⊡ ALKENES |
| ◇ TOLUENE | ✕ M−XYLENE | ✕ ACETALD |

Experimental MR [IntOH] vs *Calculated MR [IntOH] (ppt−min/ppmC)*

Low NOx Lumped Surrogate

☉ CO	▲ ALKANES	⊡ ALKENES
Y BENZENE	✕ TOLUENE	✕ M−XYLENE
+ ACETALD	◇ FORMALD (IR)	

Experimental MR [IntOH] vs *Calculated MR [IntOH] (ppt−min/ppmC)*

Figure 53. Plots of experimental <u>vs</u> calculated 6-hour IntOH mechanistic reactivities for the various types of reactivity experiments. Note that the reactivities are given on a per-carbon basis.

significant discrepancies were observed. As discussed above, one low NO_x reactivity characteristic observed for most VOCs is an inhibition of IntOH by the end of the run. The model gave good predictions of this low NO_x IntOH inhibition in the cases of CO, ethene, <u>trans</u>-2-butene, and acetaldehyde, but slightly underpredicted the IntOH inhibition for n-butane, n-octane and propene, slightly overpredicted it for toluene and one of the m-xylene experiments, and significantly overpredicted it for benzene and the other m-xylene run. The $d(O_3$-NO) incremental and mechanistic reactivities were reasonably well predicted in most cases except perhaps for the t=1 hour points for propene (which may be due to problems with the t=1 propene data), and a slight underprediction of the small $d(O_3$-NO) inhibition caused by acetaldehyde. The only discrepancy which is clearly outside the uncertainty of the data is the significant overprediction of the IntOH inhibition observed in the benzene experiment.

Ethene Surrogate

○ CO △ ALKANES ⊡ PROPENE
◇ T-2-BUTE ✕ M-XYLENE

High NOx Lumped Surrogate

○ CO △ ALKANES ⊡ ALKENES
◇ TOLUENE ✕ M-XYLENE ✕ ACETALD
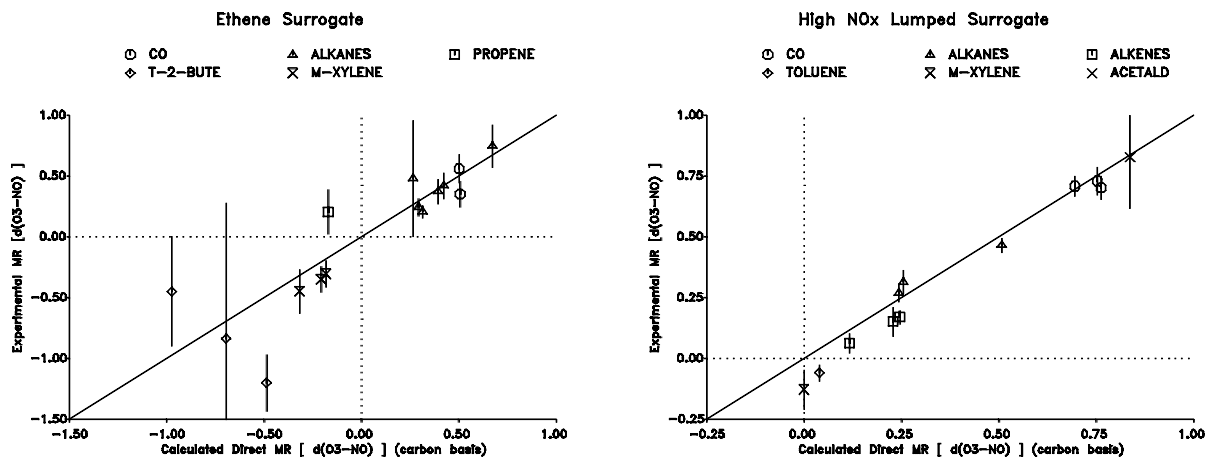
Figure 54. Plots of experimental $\underline{vs}$ calculated 6-hour direct $d(O_3-NO)$ mechanistic reactivities for the various types of high NO_x reactivity experiments. Note that the reactivities are given on a per-carbon basis.

The mechanistic implications of the results of the modeling of these and the other reactivity experiments are discussed in the following section.

VI. DISCUSSION

A.   Effect of ROG Surrogate on Reactivity

A summary of the major experimental results using different ROG surrogates obtained from this and our previous work (Carter et al., 1993a) is given in Table 15. The results are given in terms of mechanistic reactivities for several reasons. First, it allows mechanistic effects for VOCs with different reaction rates to be directly compared. Otherwise, the significant differences in the VOCs in terms of their reaction rates will dominate the results. In addition, it allows mechanistic effects of a given VOC to be compared for experiments with differing radical levels. All else being equal, the incremental reactivity of a VOC will increase if the radical levels in the experiment increases, because more of the VOC will react during the experiment. Use of mechanistic reactivities allows this purely kinetic effect to be factored out when assessing the effect of the ROG on reactivity. Although the effects of differing VOC reaction rates and environmental radical levels are obviously important, they can be adequately predicted for VOCs whose reaction rates are known if the model for base case conditions adequately simulates the environment's radical levels. Factoring out kinetic effects by examining mechanistic reactivities provides information on whether other, perhaps less obvious, mechanistic effects are also important.

The high NO_x mechanistic reactivities can be further broken down into direct and indirect mechanistic reactivities. The former provides an estimate of the number of molecules of NO oxidized and O_3 formed caused directly by the reactions of the VOC its oxidation products, per molecule of VOC reacting. The latter refers to the effect of the test VOC's reactions on the amount of NO oxidized and O_3 formed from the reactions of the other VOCs' present, i.e., from the reactions of the components of the base ROG mixture. Under high NO_x conditions, the indirect reactivity is due entirely to the effect of the VOC on radical levels, which in turn affects how much of the components of the base ROG are reacting to oxidize NO or form ozone. The estimates of direct and indirect mechanistic reactivities in the various experiments are included in Table 15, and a comparison of the averages of these data for the various VOCs and ROG surrogates in the high NO_x experiments are shown on Figure 55.

Table 15 and Figure 55 show that, at least for high NO_x conditions and for those compounds where sufficient useful direct reactivity data could be obtained, the nature of the base ROG surrogate has no significant effect on direct reactivity. This is as expected, since the radicals formed in a VOC's oxidations which cause NO oxidation generally react primarily with NO_x, and not with radicals from other VOCs, at least under conditions when ozone formation is occurring. On the other hand, Table 15 and Figure 55 show that, for some VOCs at least, the indirect reactivity can depend significantly on the base ROG surrogate. In general, the indirect reactivities tend to have higher magnitudes,

119

Table 15. Summary of selected results for reactivity experiments using different ROG surrogates and NOₓ levels.

Experiment [a]				Added (ppm)	Reacted (ppm)	Incr. React'y (mol O3-NO/ mol added)	Mech. React'y (mol O3-NO/mol reacted)		
NOx	Surg	Run	Hr.				Overall	Indirect	Direct
Carbon Monoxide									
Hi	Mini	E418	6	110.	0.662 ± 6%	0.0039 ±16%	0.6 ± 0.1	-0.2 ± 0.1	0.8 ± 0.1
Hi	Mini	E418	6	110.	0.662 ± 6%	0.0039 ±16%	0.6 ± 0.1	-0.2 ± 0.1	0.8 ± 0.1
Hi	Mini	E416	6	130.	0.726 ± 6%	0.0048 ±11%	0.9 ± 0.1	-0.1 ± 0.1	0.9 ± 0.1
Hi	Ethe	E487	3	107.	0.326 ±30%	0.0035 ±11%	1.1 ± 0.4	0.1 ± 0.4	1.2 ± 0.5
Hi	Ethe	E487	3	107.	0.326 ±30%	0.0035 ±11%	1.1 ± 0.4	0.1 ± 0.4	1.2 ± 0.5
Hi	Ethe	E483	3	155.	0.461 ±31%	0.0031 ± 9%	1.0 ± 0.3	-0.1 ± 0.3	1.1 ± 0.4
Hi	Surg	D014	6	155.	1.209 ± 5%	0.0043 ± 8%	0.5 ± 0.0	-0.2 ± 0.0	0.7 ± 0.0
Hi	Surg	D015	4	161.	1.100 ± 4%	0.0047 ± 6%	0.7 ± 0.1	0.0 ± 0.0	0.7 ± 0.0
Hi	Surg	D016	6	74.2	0.684 ± 4%	0.0059 ±10%	0.6 ± 0.1	-0.1 ± 0.1	0.7 ± 0.1
Hi	Surg	D020	6	103.	0.869 ± 4%	0.0055 ± 7%	0.7 ± 0.1	0.0 ± 0.0	0.7 ± 0.0
Lo	Surg	D029	6	85.8	0.659 ± 4%	0.0024 ±15%	0.3 ± 0.1	[b]	[b]
Ethane									
Hi	Mini	E235	6	43.7	0.306 ± 6%	0.0058 ±26%	0.8 ± 0.2	-0.6 ± 0.3	1.4 ± 0.3
Hi	Ethe	E506	3	49.7	0.181 ±29%	0.0044 ±20%	1.2 ± 0.4	-0.2 ± 0.5	1.5 ± 0.8
n-Butane									
Hi	Mini	E224	6	9.76	0.309 ±17%	0.0269 ±26%	0.8 ± 0.3	-1.4 ± 0.4	2.2 ± 0.4
Hi	Ethe	E488	3	10.31	0.221 ±45%	0.0242 ±17%	1.1 ± 0.5	-0.6 ± 0.6	1.7 ± 0.9
Hi	Ethe	E484	3	15.2	0.341 ±43%	0.0314 ± 9%	1.4 ± 0.6	-0.2 ± 0.4	1.7 ± 0.8
Hi	Surg	D019	6	6.48	0.441 ± 5%	0.0808 ± 9%	1.2 ± 0.1	-0.7 ± 0.1	1.9 ± 0.1
Lo	Surg	D031	6	5.48	0.281 ± 7%	0.0332 ±17%	0.6 ± 0.1	[b]	[b]
n-Hexane									
Hi	Ethe	D072	6	2.88	0.166 ±73%	-0.0375 ±38%	-0.6 ± 0.5	-3.6 ± 3.4	2.9 ± 2.9
n-Octane									
Hi	Mini	E239	6	1.55	0.064 ±28%	-0.243 ±18%	-5.9 ± 2.0	-9.7 ± 3.2	3.5 ± 1.4
Hi	Mini	E237	6	1.66	0.098 ±19%	-0.235 ±17%	-4.0 ± 1.0	-5.9 ± 1.5	1.9 ± 0.8
Hi	Ethe	E472	6	1.60	0.278 ±17%	-0.135 ±26%	-0.8 ± 0.2	-2.6 ± 0.6	1.7 ± 0.4
Hi	Ethe	E474	6	2.27	0.286 ±24%	-0.0839 ±32%	-0.7 ± 0.3	-2.6 ± 0.7	2.0 ± 0.6
Hi	Surg	D024	6	1.10	0.216 ±14%	0.162 ±22%	0.8 ± 0.2	-1.7 ± 0.3	2.5 ± 0.4
Hi	Surg	D070	6	0.74	0.176 ±12%	0.174 ±26%	0.7 ± 0.2	-1.4 ± 0.2	2.2 ± 0.3
Lo	Surg	D037	6	1.12	0.201 ±17%	0.0524 ±46%	0.3 ± 0.1	[b]	[b]
Lo	Surg	D071	6	0.647	0.142 ±12%	0.0727 ±57%	0.3 ± 0.2	[b]	[b]
Ethene									
Hi	Mini	E203	6	0.21	0.086 ±29%	0.912 ±35%	2.3 ± 1.0	2.0 ± 1.2	[c]
Hi	Mini	E199	6	0.38	0.172 ±20%	1.14 ±17%	2.5 ± 0.6	1.9 ± 0.8	[c]
Hi	Surg	D017	6	0.60	0.340 ± 4%	0.673 ±11%	1.2 ± 0.1	0.9 ± 0.1	0.3 ± 0.1
Lo	Surg	D038	6	0.65	[d]	0.0864 ±47%		[b]	[b]
Propene									
Hi	Surg	E106	6	0.081	0.057 ± 7%	2.61 ±13%	3.7 ± 0.5	2.1 ± 0.6	1.6 ± 0.6
Hi	Surg	E108	9	0.085	0.057 ± 5%	1.98 ±16%	3.0 ± 0.5	1.5 ± 0.6	1.6 ± 0.6
Hi	Surg	E118	6	0.148	0.108 ± 6%	1.63 ±12%	2.2 ± 0.3	1.3 ± 0.5	1.0 ± 0.5
Hi	Ethe	E500	3	0.21	0.121 ± 4%	1.53 ±13%	2.7 ± 0.4	0.1 ± 1.0	2.3 ± 1.2
Hi	Ethe	E496	3	0.30	0.222 ± 3%	1.58 ± 8%	2.2 ± 0.2	1.6 ± 0.7	0.1 ± 0.9
Hi	Surg	D018	6	0.35	0.348 ± 2%	0.950 ±13%	1.0 ± 0.1	0.8 ± 0.1	0.2 ± 0.1
Lo	Surg	D032	6	0.30	0.303 ± 2%	0.007 ±0.08	0.0 ± 0.1	[b]	[b]

Table 15 (continued)

Experiment [a]				Added (ppm)	Reacted (ppm)	Incr. React'y (mol O3-NO/ mol added)		Mech. React'y (mol O3-NO/mol reacted)		
NOx	Surg	Run	Hr.					Overall	Indirect	Direct

trans-2-Butene

Hi	Mini	E309	6	0.06	0.068 ±11%	5.47	±21%	5.5 ± 1.2	4.2 ± 1.5	[c]
Hi	Mini	E307	6	0.08	0.086 ±35%	5.09	±38%	5.1 ± 1.9	4.5 ± 2.0	[c]
Hi	Ethe	E501	3	0.06	0.066 ± 2%	7.92	± 8%	7.9 ± 0.6	5.6 ± 2.3	[c]
Hi	Ethe	D043	3	0.09	0.097 ± 2%	6.82	± 5%	6.8 ± 0.4	6.1 ± 2.9	[c]
Hi	Ethe	E493	3	0.14	0.142 ± 2%	5.07	± 6%	5.1 ± 0.3	5.0 ± 1.4	[c]
Hi	Surg	D021	4	0.32	0.320 ± 2%	1.42	± 8%	1.4 ± 0.1	0.6 ± 0.1	0.8 ± 0.1
Hi	Surg	D069	5	0.19	0.190 ± 2%	1.65	±12%	1.6 ± 0.2	1.0 ± 0.2	0.6 ± 0.2
Lo	Surg	D033	6	0.15	0.154 ± 2%	-0.14	±0.2	-0.1 ± 0.2	[b]	[b]

Benzene

Hi	Mini	E265	6	5.78	0.357 ±14%	0.0479	±24%	0.8 ± 0.2	[b]	[b]
Hi	Mini	E263	6	6.86	0.447 ±11%	0.0224	±44%	0.3 ± 0.2	[b]	[b]
Lo	Surg	D039	6	7.39	0.296 ± 5%	-0.0110	±30%	-0.3 ± 0.1	[b]	[b]

Toluene

Hi	Mini	E101	6	0.170	0.030 ±16%	1.22	±13%	6.9 ± 1.4	5.9 ± 1.5	0.8 ± 1.2
Hi	Mini	E103	6	0.174	0.034 ±15%	1.34	±11%	7.0 ± 1.3	5.3 ± 1.4	1.6 ± 1.3
Hi	Surg	D023	3	0.57	0.108 ±14%	0.539	±10%	2.8 ± 0.5	1.9 ± 0.4	1.0 ± 0.4
Lo	Surg	D030	6	1.13	0.201 ±16%	-0.0803	±26%	-0.5 ± 0.1	[b]	[b]

m-Xylene

Hi	Mini	E301	6	0.05	0.033 ±20%	6.16	±23%	9.9 ± 2.8	7.7 ± 3.2	[c]
Hi	Mini	E196	6	0.05	0.034 ±11%	3.41	±36%	5.7 ± 2.1	5.4 ± 2.8	[c]
Hi	Mini	E344	6	0.08	0.049 ±33%	5.70	±23%	9.3 ± 3.3	[e]	[e]
Hi	Ethe	E478	3	0.09	0.045 ± 5%	4.09	±11%	8.7 ± 1.0	7.4 ± 2.7	[c]
Hi	Ethe	E499	2	0.14	0.046 ± 8%	2.17	± 8%	7.0 ± 0.8	7.0 ± 3.1	[c]
Hi	Ethe	E477	3	0.17	0.098 ± 4%	4.22	± 6%	7.5 ± 0.5	6.0 ± 1.8	[c]
Hi	Surg	D025	6	0.08	0.066 ± 3%	3.46	±15%	4.4 ± 0.7	5.4 ± 0.6	-1.0 ± 0.6
Hi	Surg	D068	5	0.06	0.043 ± 3%	3.74	±14%	5.6 ± 0.8	5.0 ± 0.8	0.6 ± 0.9
Lo	Surg	D035	6	0.10	0.069 ± 3%	-0.510	±46%	-0.8 ± 0.4	[b]	[b]
Lo	Surg	D067	6	0.17	0.107 ± 6%	-0.347	±40%	-0.6 ± 0.2	[b]	[b]

Formaldehyde

Hi	Mini	E352	6	0.10	[d]	2.37	±27%			
Hi	Mini	E357	6	0.26	[d]	1.35	±19%			
Hi	Ethe	E468	3	0.10	[d]	1.44	±24%			
Hi	Ethe	E470	3	0.26	[d]	1.94	± 8%			
Hi	Ethe	E489	3	0.28	[d]	1.66	± 9%			
Hi	Surg	D022	6	0.40	[d]	0.754	±13%			
Lo	Surg	D036	6	0.24	[d]	0.05	±0.11			

Acetaldehyde

Hi	Mini	E335	6	0.69	0.261 ± 7%	0.226	±43%	0.6 ± 0.3	-0.9 ± 0.4	1.6 ± 0.3
Hi	Mini	E338	6	1.31	0.444 ± 8%	0.113	±46%	0.3 ± 0.2	-0.9 ± 0.2	1.3 ± 0.2
Hi	Surg	D065	6	1.53	0.377 ±24%	0.148	±16%	0.6 ± 0.2	-1.1 ± 0.3	1.7 ± 0.4
Lo	Surg	D066	6	1.62	0.247 ±40%	-0.0345	±44%	-0.2 ± 0.1	[b]	[b]

[a] Codes for NO$_x$ conditions: "Hi" = maximum reactivity; "Lo" = NO$_x$-limited O$_3$. Codes for base ROG
     surrogates: "Mini" = Mini-surrogate (from Carter et al., [1993a]), "Ethe" = ethene surrogate;
     "Surg" = 8-component "lumped molecule" surrogate. ETC runs codes have "E" prefix; DTC runs have
     "D" prefix. Hr is hour in run where data given. Data given for t<6 hours in maximum reactivity
     experiments where the final O$_3$ appears to be nearly NO$_x$-limited, or if t=6 data missing.
[b] Methods used to estimate direct and indirect reactivities are not valid for NOx-limited
     conditions.
[c] Estimated minimum uncertainty to great to yield meaningful data.
[d] Amounts reacted could not be determined, or uncertainties too high for meaningful data.
[e] Indirect and direct reactivity results for this run appear to be anomalous

121
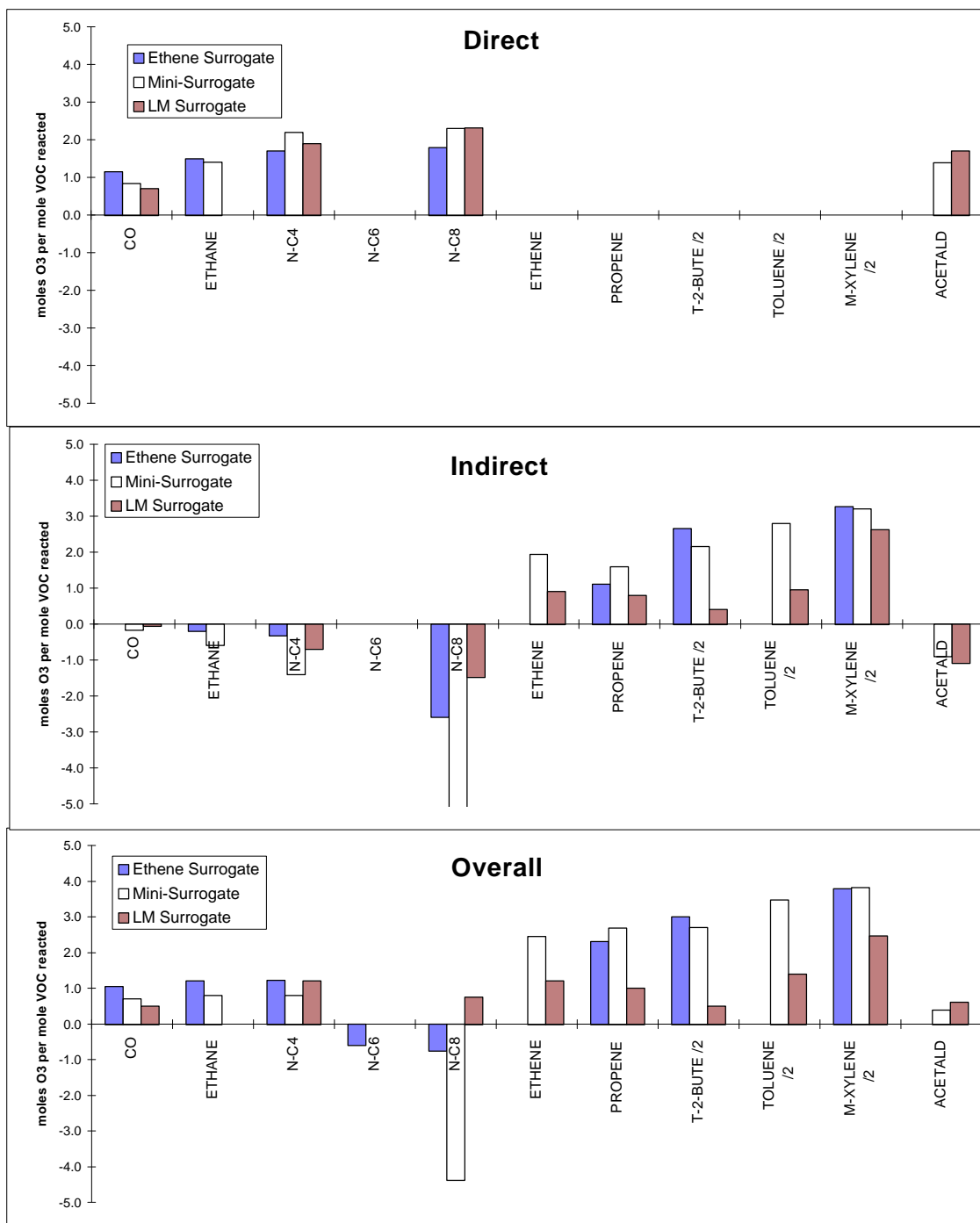
Figure 55.   Comparisons of weighed averages of the direct, indirect,
              and overall mechanistic reactivities for high NOx
              conditions for the three base ROG surrogates. The averages
              are of the data on Table 15. The units of the data are
              moles d(O3-NO) per mole VOC reacting.

both positive and negative, in the experiments using the ethene or the mini-surrogates than is the case when the full, lumped molecule, surrogate is used. For example, the radical inhibition by n-octane is much greater with the mini-surrogate, and somewhat greater with the ethene surrogate, than it is with the full surrogate. A similar effect is seen, though to a lesser extent, with n-butane and ethane, though in the case of n-butane the indirect reactivities for the ethene and the full surrogates are the essentially the same. Similarly, the positive indirect reactivities for trans-2-butene and toluene are much greater with the simpler surrogates than it is with the full surrogate, and similar results, though to a lesser extent, are seen with ethene, propene, and m-xylene. Acetaldehyde is somewhat unusual in that its indirect reactivity is essentially the same with the mini- and full surrogates.

Thus the effect of the base ROG on the VOC's indirect incremental reactivity is the primary factor affecting a how the base ROG affects the VOC's overall incremental reactivity under high NO_x conditions. Under such conditions, the indirect reactivity of a VOC depends on two factors: its IntOH reactivity and the $d(O_3-NO)$/IntOH ratio for the base ROG. The latter averaged 3.3, 3.2, and 2.6 x 10^4 min^{-1} for the ethene, mini-, and full surrogate base case runs, respectively. Thus the base ROG $d(O_3-NO)$/IntOH ratio is roughly equal for the two simpler surrogates, and is approximately 20% lower for the full surrogate. The difference for the full surrogate is not sufficient to explain the indirect reactivity differences for most of the VOCs. Therefore, the effect of the base ROG on the VOC's IntOH reactivity, i.e., on how the VOC affects OH radical levels, appears to be the primary factor determining the effect on overall reactivity.

In general, the use of the simpler surrogate tends to result in greater magnitudes of IntOH reactivities, whether positive or negative, than use of the more realistic lumped surrogate. In other words, the addition of VOCs cause greater changes in OH radical levels in runs with the simpler surrogates than in their addition in runs with more complex surrogates. This is probably due to species in the complex surrogate providing radicals earlier in the run than those in the simpler surrogates. In particular, the lumped surrogate contains formaldehyde and trans-2-butene, whose reactions cause relatively large radical inputs early in the experiment. The m-xylene and/or ethylene in the simpler surrogates also provide radical inputs, but generally not as much as early in the run as is the case for formaldehyde and trans-2-butene. The earlier radicals apparently make the system less sensitive to the radical input or radical inhibition caused by the addition of the test VOCs than would be the case if these early radical sources are missing.

The effects of the ROG surrogate on reactivity observed in this study are entirely consistent with the predictions of the model calculations discussed in Section II. Those calculations predicted that in general the use of the simpler ROG surrogates (i.e., ethene and the mini-surrogate) would give results which are

more sensitive to differences among VOCs than use of more realistic surrogates, and this is indeed what was observed. The model is also able to successfully simulate the results of most of the reactivity experiments, particularly for the experiments using the more complex ROG surrogate. The performance of the current mechanisms in simulating these data is discussed in more detail later.

B.   Effect of NO_x on Reactivity

As expected based on modeling studies (e.g., Carter and Atkinson, 1989), NO_x conditions were found to significantly affect VOC reactivities, both in an absolute and a relative sense. Reducing NO_x levels reduced incremental reactivities for all VOCs studied, but the amount of reduction varied greatly among the VOCs. A number of VOCs whose mechanistic reactivities were both positive and high under high NO_x conditions were found to become negative in the low NO_x experiments. This was true not only of the aromatics, but also for trans-2-butene and acetaldehyde. In the case of propene, another relatively reactive compound under high NO_x conditions, the reactivity became essentially zero in the low NO_x experiments. The incremental reactivity of formaldehyde, while still positive, was a factor of ~15 times lower than under high NO_x conditions. On the other hand, the mechanistic reactivities for ethene only reduced by a factor of five, and those for CO and the alkanes reduced by only a factor of two.

The trends observed are consistent with the expectation that low NO_x reactivities are strongly influenced by NO_x sinks in the VOCs' mechanisms. The species whose reactivities changed the most as NO_x changed were all species believed to have the most important NO_x removal processes. In the case of the aromatics, the NO_x sinks are believed to include the formation of species such as nitrophenols from the aromatic ring-retaining products, and the formation of PAN from the dicarbonyls and other fragmentation products. In the case of acetaldehyde, it is the formation of PAN. In the case of propene and trans-2-butene, it is the formation of acetaldehyde, which in turn reacts to form PAN. Ethene, CO and n-butane have relatively small NO_x sinks, and thus reducing NO_x does not cause as great a change in reactivity for those compounds. However, reactivity is still reduced because of the lower efficiency for O_3 formation under lower NO_x conditions.

The effects of VOCs on radicals would still be expected to have some effect on reactivity under low NO_x conditions, though it is clearly does not have the overriding importance it does under high NO_x conditions. For the VOCs studied here, there is no correlation between IntOH and $d(O_3-NO)$ reactivities under low NO_x conditions — the correlation coefficient for the mechanistic reactivities (incremental for formaldehyde) is -0.17. (By contrast, the correlation coefficient for the high NO_x experiments with the same ROG surrogate is 0.99.) The reduced importance of radicals under low NO_x conditions is indicated by the relatively large reduction in the formaldehyde incremental reactivity, despite the fact that it does not have significant NO_x sinks in its mechanism. This is probably also one reason the change in incremental reactivity of n-octane is not

124

as large as might be expected given the formation of alkyl nitrates in its reactions. In this case, the large radical sinks in the n-octane mechanism, which is the major factor giving it a low reactivity under high NO_x conditions, is less important in suppressing its reactivity when NO_x is lower, and this tends to counteract the relative reduction of reactivity due to n-octane's NO_x sinks.

It is interesting to note that under low NO_x conditions all the VOCs studied except for formaldehyde suppressed radical levels. The high radical suppression by acetaldehyde can be attributed to the fact that most of its reaction with OH radicals involves formation of PAN, which is a radical sink process. In the case of VOCs with NO_x sinks, such as aromatics, radical suppression would be expected because termination by radical-radical reactions become more important when NO_x runs out. However, in the case of the other VOCs, the suppression is apparently simply due to the fact that the VOC is promoting ozone. Otherwise, it would be difficult to understand why CO, which has neither radical nor NO_x sinks in its mechanism, is suppressing IntOH such a large extent. This general suppression might be due to the higher O_3 levels caused by the test VOC causing lower steady state NO levels, which means that radical propagation reactions of peroxy radicals with NO are less competitive with termination by radical + radical reactions.

C.   Mechanism Evaluation Results

With a few exceptions, discussed below, the current detailed mechanism performs remarkably well in simulating the reactivity results in this study. The most concise indication of the ability of the mechanism to simulate the various measured components of reactivity is obtained from Figures 52-54, above. The major effects on reactivity of changing the ROG surrogate and the NO_x levels, discussed above, are all successfully simulated by the model.

There were, however, a few cases of poor model performance suggesting possible problems in the mechanism. The poor model performance in simulating the low NO_x IntOH reactivity of benzene and to a lesser extent the other aromatics suggest problems in some fundamental aspect of the aromatics mechanisms. A similar problem was seen in the model simulation of the IntOH reactivity under high NO_x conditions with the Phase I mini-surrogate (Carter et al., 1993a), where a compensating error in the prediction of the direct reactivity caused a fairly good prediction of overall reactivity. However, the model is successful in simulating the $d(O_3-NO)$ reactivities of toluene and m-xylene under all conditions studied, and in simulating their IntOH reactivities reasonably well under high NO_x conditions.

In general, the model performed better in simulating the reactivities in the experiments with the complex surrogate than it did in the ethene surrogate runs. This is despite the uncertainties in the mechanism for some of the components of the complex surrogate, and despite the fact that the model tended to underpredict the rate of ozone formation in the base case high NO_x surrogate

125

experiments. One part of the reason for this is that the system with the more complex surrogate appears to be less affected by radical initiation and inhibition effects of the added VOCs than is the case with ethene or the mini-surrogate. Thus, the more complex surrogate is less sensitive to mechanism differences among VOCs, so errors in these mechanisms will have less of an effect on the results. In addition, errors in the base case mechanisms of the components of the more complex surrogate may have less of an effect than errors in the base mechanisms for simpler surrogates, because with a complex mixture no single compound in the mixture tends to dominate the results.

The most serious discrepancies observed in the ethylene surrogate experiments were the predictions of the reactivities of n-octane and formaldehyde. In particular, the model overpredicted the initiation caused by adding n-octane, and overprotected the initiation caused by adding formaldehyde. There may be slight overpredictions in the high NO_x lumped surrogate runs with these compounds, but in these cases the model predictions are close to the experimental uncertainty ranges.

The problem with n-octane is difficult to rationalize, especially since the model successfully simulated the reactivity of n-octane in the mini-surrogate experiments (Carter et al., 1993a). There is an indication of a similar problem in the case of the predictions of the n-butane and n-hexane reactivities in the ethene surrogate runs, though the discrepancy for n-hexane is less than that for n-butane, which is not the trend one would expect. Unfortunately, the IntOH data in the ethene surrogate experiments are not sufficiently precise to clearly indicate whether the problem is due to problems in predicting direct or indirect reactivities. The model predictions are not inconsistent with the direct mechanistic reactivity data, but the uncertainty of the latter, due to the combined uncertainties in the IntOH data and the amounts of n-octane reacting, are such that this is not particularly meaningful.

However, the problem is most likely with the amount of radical inhibition caused by n-octane, i.e., with the indirect reactivity. Adjusting the n-octane mechanism by reducing the alkyl nitrate yield from ~33% to ~25% causes the model to give good fits to all the reactivity data in the ethene surrogate experiments. However, this adjusted n-octane model overpredicts the $d(O_3-NO)$ reactivity of n-octane in the high NO_x lumped surrogate run, and somewhat underpredicts its $d(O_3-NO)$ inhibition in the mini-surrogate runs. This adjusted mechanism is also inconsistent with the experimentally observed ~33±3% octyl nitrate yields reported by Atkinson et al. (1982), which is used as the basis for the current mechanism. This needs further investigation, including an independent confirmation of the octyl nitrate yields reported by Atkinson et al. (1982).

The overprediction by the model of the incremental reactivity of formaldehyde in both the ethene and the mini-surrogate experiments is disturbing because the atmospheric chemistry of formaldehyde has been considered to be

reasonably well established. The discrepancy appears to be the greatest in the run with the smallest amount of added formaldehyde, and (for both ethene and the mini-surrogate) is relatively greater earlier in the runs than it is later. In view of the consistent results with the quite different base ROG surrogates, it is unlikely to be due to a problem in the base ROG mechanism, a possibility considered in the Phase I report (Carter et al., 1993a). A slight overprediction of the $d(O_3-NO)$ formation rate and formaldehyde consumption rates are observed in model simulations of formaldehyde - NO_x experiments carried out for this program, though the extent of the model discrepancy is not as great as indicated by the incremental reactivity results. This is discussed in more detail elsewhere (Carter et al., 1995a).

D.   Correlations Between Experimental and Atmospheric Reactivities

It is of interest to see how well experimental incremental reactivities can correlate with those calculated for the atmosphere. In Section II, we used model simulations to predict how well mechanistic reactivities measured in environmental chamber experiments would correlate with those in the atmosphere. A fair correlation was obtained for high NO_x maximum reactivity conditions, but no correlation was obtained for NO_x-limited conditions. However, better correlations might be expected for incremental reactivities, because of the large differences in VOC's reaction rates, which are not taken into account in correlations of mechanistic reactivities, would similarly affect incremental reactivities under both conditions. The best correlation would be expected for experiments with the most realistic base ROG mixtures, and as discussed in Section II the lumped surrogate appears to be sufficiently realistic for this purpose. Furthermore, since the model gives good simulations of the reactivities of the VOCs studied using this surrogate, one might expect the atmospheric model simulations to be reasonably accurate in terms of the aspects of the chemical mechanism which affect predictions of reactivity.

Figure 56 shows plots of the experimental per-carbon incremental reactivities of the VOCs studied against those calculated for the atmosphere for similar NO_x conditions. The experimental data is from the runs using the lumped surrogate. The high NO_x experimental reactivities are compared with those in the Maximum Incremental Reactivity (MIR) scale, since the MIR scale is based on atmospheric reactivities under high NO_x conditions (Carter, 1994). The low NO_x experimental reactivities are compared with those in the Equal Benefit Incremental Reactivity (EBIR) scale, which is a scale based on atmospheric reactivities under NO_x-limited conditions. (The EBIR scale was chosen rather than the MOIR scale — which represents intermediate NO_x conditions which are optimum for O_3 formation — because it corresponds more closely to the conditions of the low NO_x experiments. However, except for toluene, which has a relatively low EBIR reactivity, EBIR and MOIR reactivities are highly correlated [Carter, 1994].)

High NOx

○ CO △ ALKANES ⊡ ALKENES
◇ AROMATICS ✕ FORMALD ✕ ACETALD
—— Atm = 6.26 x Chamber

Atmospheric Reactivity (MIR)

5.

4.

3.

2.

1.

0.

0.0   0.2   0.4   0.6   0.8
Chamber Reactivity

Low NOx

○ CO △ ALKANES ⊡ ALKENES
◇ AROMATICS ✕ FORMALD ✕ ACETALD

Atmospheric Reactivity (EBIR)

0.8

0.6

0.4

0.2

0.0

-0.05 -0.04 -0.03 -0.01 0.00 0.01 0.03 0.04 0.06
Chamber Reactivity
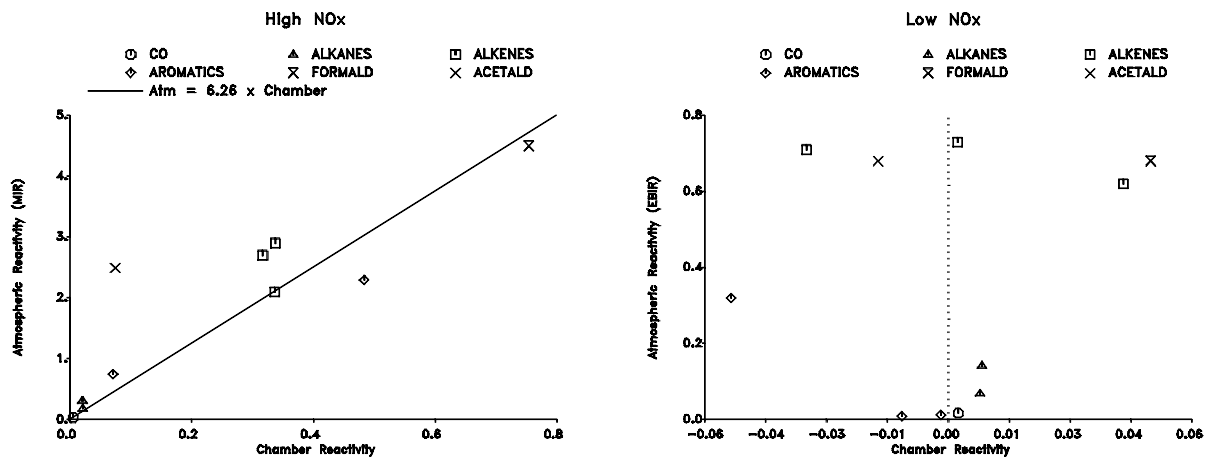
Figure 56.   Plots of atmospheric incremental reactivities (carbon basis) against incremental reactivities in the environmental chamber experiments using the lumped surrogate. High NO_x chamber reactivities are plotted against atmospheric reactivities in the MIR scale, and low NO_x chamber reactivities are plotted against atmospheric reactivities in the low NO_x "Equal Benefit Incremental Reactivity" scale.

Figure 56 shows that there is a fair correlation between the high NO_x experimental and atmospheric MIR reactivities of all the VOCs studied except for acetaldehyde. Note, however, that the incremental reactivities in the chamber have much lower magnitudes than those in the atmosphere, the best fit line shown on the figure indicates that they are lower by over a factor of ~6. Although the correlation coefficient excluding acetaldehyde is 96% (it is 88% with acetaldehyde), using the best fit line only predicts the incremental reactivities to within ±50% in some cases. Therefore, although chamber experiments can indeed give an indication of atmospheric reactivity under high NO_x conditions without having to rely on modeling, the estimates cannot be considered to be highly precise.

The poor correlation in the case of acetaldehyde cannot be attributed to problems with the model because it is reasonably successful in simulating acetaldehyde reactivity experiments. Part of the problem may be the light source; the photolysis rate of acetaldehyde relative to that of NO_2 is calculated to be almost 3 times slower in the chamber experiment than in the atmosphere. However, a reasonably good correlation was obtained for formaldehyde, which photolyzes ~2 times slower relative to NO_2. Another probable factor is the fact that (unlike the model simulations of the chamber experiments in Section II) the experiments do not represent true incremental reactivities, since finite amounts of test compounds had to be added to yield measurable results.

Figure 56 also shows that there is essentially no correlation between low NO_x reactivities in the chamber and those in the atmosphere. This is despite the fact that the model gave quite good predictions of the low NO_x reactivities in the chamber. This is consistent with the model predictions given in Section II. As indicated there, this is attributed to the fact that low NO_x O_3 reactivities are determined by the interactions of several different factors, whose relative importance are apparently quite different in the chamber than in the atmosphere. It may be possible to design a chamber experiment where somewhat better low NO_x reactivity correlations could be obtained, though it unclear whether it would be worth the probably considerable effort and expense required to do this. Model simulations would probably be the only practical way to estimate low NO_x reactivities for the foreseeable future.

VII. CONCLUSIONS

This study, in conjunction with our Phase I work, has provided a large experimental data base on VOC reactivity. The Phase I work has provided information concerning reactivities of a wide variety of compounds under a single set of conditions, and this work has provided information concerning a smaller number of species under more varied conditions. These new data are useful for assessing how the presence of other pollutants in the atmosphere affect a VOC's reactivity, and for evaluating how well current photochemical models can predict these effects. This work has also provided useful information on the relative utility of various types of experimental data in reactivity assessment and mechanism evaluation.

Both model simulations and experimental data have shown that the presence of other VOC pollutants, referred to as the "base ROG", can significantly affect a VOC's ozone reactivity. For example, the model predicted, and the experimental data confirmed, that the incremental reactivity of n-octane could change sign, and the absolute reactivities of species such as alkenes, aromatics, and formaldehyde could change significantly, depending on the mixture used to represent the base ROG. VOCs were found to have much smaller differences in mechanistic reactivities (reactivities with effects of the VOC's reaction rates factored out) when reacting in the presence of a more complex mixture designed to represent ambient ROG pollutants than when reacting in the presence of the 3-component "mini-surrogate" used in our Phase I study, or when reacting in the presence of ethylene alone. This is attributed to species in the more complex mixture, such as formaldehyde and (perhaps to a lesser extent) internal alkenes, which provide radical sources early in the irradiations, and tend to make the system less sensitive to the radical input or termination processes caused by the test VOC.

On the other hand, model simulations showed that it is probably not necessary to use a highly complex mixture to adequately represent the effects of other ROG pollutants in experimental studies of incremental reactivity. Use of a simple 8-component mixture, containing approximately the level of chemical detail as incorporated in condensed "lumped molecule" mechanisms in airshed models, was calculated to provide indistinguishable reactivity results in chamber experiments as use of a ambient ROG mixture containing the full set of compounds measured in the atmosphere. But simplifying this 8-component mixture further was found to begin to have non-negligible effects on reactivity. The mixture was derived based on the amounts and types of reactive molecules present; representation of all the carbon present was found not to be important. It can be argued that this result may be an artifact due to the chemical mechanism having a comparable degree of condensation as the 8-component mixture. However, the chemical mechanism used in this assessment had sufficient detail to represent many, though not all, of the chemical complexities in the ambient mixture. In

any case, if there are any differences in reactivity in experiments using a more complex ROG surrogate than the 8-component mixture, they clearly cannot be accounted for by the present generation of detailed mechanisms.

Using a realistic ROG surrogate is obviously necessary if experimental reactivity data are to correspond to reactivities in the atmosphere. However, it is not sufficient. Model calculations showed that even if the ambient mixture itself is used as the ROG surrogate, the mechanistic reactivities in chamber studies would not necessarily correspond to those in the atmosphere. This was confirmed by the experimental data. The extent to which chamber reactivities correlate with those in the atmosphere depended significantly on NO_x conditions. Under high NO_x conditions, experimental incremental reactivities correlate moderately well with atmospheric reactivities in the MIR scale, though the correlation was poor for acetaldehyde, and the correlation with the chamber data could only predict the atmosphere reactivities for the other VOCs to within ±50%. Under low NO_x conditions, there was no correlation at all between atmospheric reactivity and reactivity in the chamber experiments. This was true whether using real chamber data or chamber data simulated by the model. Reactivities under low NO_x conditions are influenced by differing and often opposing factors, and apparently balances among these factors are quite different in the chamber experiments than in the atmosphere.

It may be possible someday to design an experimental system which gives better correlations between experimental and atmospheric reactivities, but we suspect it would be extremely difficult and expensive, and may yield data with large experimental uncertainties. In the meantime, we must rely on model simulations to predict reactivities in the atmosphere. The role of the chamber data is thus not to directly measure atmospheric reactivity, but rather to evaluate and if necessary calibrate the models which must be used for this purpose.

Experiments with both realistic and simplified ROG surrogates are necessary for an adequate evaluation of the ability of models to predict reactivity. Use of realistic surrogates are obviously necessary to test the ability of the mechanism to simulate reactivities in chemically realistic conditions. However, experiments with simpler surrogates are more sensitive to differences among VOCs, particularly in terms of their effects on radical levels. This means that model simulations of those experiments would be more sensitive to errors in the mechanisms of the VOCs. This is consistent with the results of this study, where in general the mechanism performed better in simulating reactivity in the experiments using the more complex surrogate than it did in the experiments using the mini-surrogate or ethylene alone.

The experimental data in this study confirmed the model predictions concerning the importance of NO_x in affecting a VOC's incremental reactivity. As expected, the incremental and mechanistic reactivities of all VOCs were

reduced under low NO_x conditions. As also expected, this reduction was the greatest for VOCs, such as aromatics, acetaldehyde, and the higher alkenes, which are believed to have significant NO_x sinks in their mechanisms. All these NO_x sink species were found to have negative reactivities in our low NO_x experiments. This includes species, such as alkenes and acetaldehyde, which are calculated to have positive reactivities under low NO_x conditions in the atmosphere (Carter, 1993, 1994). Thus, low NO_x chamber reactivity experiments appear to be highly sensitive to effects of NO_x sinks in VOC's mechanisms — much more so than is apparently the case in the atmosphere. This high sensitivity may be the cause of the poor correlation between low NO_x chamber data and atmospheric reactivities. However, this also means that the chamber data should provide a highly sensitive test to this aspect of the mechanism.

The current detailed chemical mechanism was found to perform remarkably well in simulating the reactivities of the VOCs with the realistic 8-component surrogate, both under high and low NO_x conditions. An exception was that the model did not correctly predict the effects of aromatics on radical levels under low NO_x conditions. The model performance was more variable in simulating the experiments with the highly simplified (ethylene only) surrogate, though the observed reactivity trends were correctly predicted. The greater variability is attributable in part to the greater sensitivity of the simpler systems to mechanism differences, as indicated above. However, it can also be attributable to the greater sensitivity of simulations of the ethene reactivity experiments to uncertainties in reaction conditions and the ethene mechanism. With more base ROG components present, errors in the mechanisms and amounts of each individual component becomes relatively less important in affecting the result.

In our previous study, we found that we could not simulate all the base mini-surrogate experiments with a single version of the m-xylene mechanism. That problem has now apparently been resolved in the process of correcting our chamber data base and revising our chamber effects models. It was also found that the ability of the model to simulate these experiments was dependent on the temperature in these runs, which was variable. The inability of the model to simulate temperature effects is considered in more detail elsewhere (Carter et al., 1995a).

Predictions of formaldehyde reactivity continues to be a problem with the model. The model was found previously to overpredict formaldehyde's reactivity in the mini-surrogate. Similar results were obtained using the ethylene surrogate. Thus, the discrepancy is unlikely to be due to a problem with the base ROG mechanism, unless it is a problem with ethylene. On the other hand, the model discrepancy was not large in simulating formaldehyde's reactivity in the presence of the more complex surrogate. Thus, the practical effect of this discrepancy in simulation of realistic mixtures may not be large. However, in view of the fundamental importance of formaldehyde, it clearly needs to be resolved.

The model significantly overpredicted the ozone inhibition caused by adding n-octane to the ethene surrogate runs, suggesting a potential problem with the higher alkane mechanism which was not indicated by previous data. Better fits to the ethene data are obtained if it is assumed the octyl nitrate yields are lower than indicated by data from a single laboratory study, though the fits to the more complex surrogate data are made somewhat worse. This needs further study, including confirmation of the nitrate yields from the C_{8+} alkanes, which are highly sensitive parameters affecting predictions of alkane reactivity.

While problems and uncertainties with the aromatics mechanisms remain, and the continuing discrepancies with formaldehyde and the new one with n-octane are a concern, the results of this study generally give a fairly optimistic picture of the ability of the model to simulate reactivities under atmospheric conditions. This optimism is in part due to the fact that systems with realistic mixtures tend to be less sensitive to errors in the mechanisms than systems that are perhaps most useful for mechanism evaluation. However, one would clearly have more confidence in the fundamental validity of reactivity predictions if the model could satisfactorily predict reactivities in simple as well as complex chemical systems. The data obtained thus far indicate that if the model can simulate reactivity with simple ROG surrogates, it should be able to do so in the more realistic chemical system.

Although this study, in conjunction with our Phase I work, has provided a large experimental data base on VOC reactivity, it is not comprehensive. For example, only 9 or 10 different VOCs have been studied using the realistic surrogate. The mini-surrogate data indicated problems with the model in simulating reactivities of branched alkanes and of aromatic isomers not studied in this work, and information is needed concerning how these problems affect predictions of reactivities in atmospheric systems. We believe the experiments with the simplified surrogates provide the most useful information for mechanism testing. Therefore, it is important that the data base of such experiments be comprehensive and of high quality. While the number of VOCs studied in Phase I study was fairly extensive, because of experimental problems the data for some was of low precision or quality. In addition, only one branched alkane was studied, and the model performed poorly in simulating its reactivity and had to be adjusted. The dividable chamber constructed under SCAQMD funding for this program was found to yield significantly more precise reactivity data than has been obtained previously, and could significantly improve the quality as well as the completeness of this data base. No information has been obtained concerning the effect of temperature on reactivity, and there is only limited information concerning the effects of using artificial light sources. The issues of temperature and light source effects, and other fundamental data needs for mechanism evaluation, are discussed in more detail in a separate report (Carter et al., 1995a).

VIII. REFERENCES

Atkinson, R. (1989): "Kinetics and Mechanisms of the Gas-Phase Reactions of the Hydroxyl Radical with Organic Compounds," J. Phys. Chem. Ref. Data, Monograph no 1.

Atkinson, R. (1990): "Gas-Phase Tropospheric Chemistry of Organic Compounds: A Review," Atmos. Environ., 24A, 1-24.

Atkinson, R. (1994): "Gas-Phase Tropospheric Chemistry of Organic Compounds," J. Phys. Chem. Ref. Data, Monograph No. 2.

Atkinson, R., S. M. Aschmann, W. P. L. Carter, A. M. Winer, and J. N. Pitts, Jr., (1982): "Alkyl Nitrate Formation from the NO_x-air Photooxidations of C_2-C_8 n-alkanes," J. Phys. Chem., 86, 4563-4569.

Atkinson, R. and S. M. Aschmann (1993): "OH Radical Production from the Gas-Phase Reactions of O_3 with a Series of Alkenes under Atmospheric Conditions," Environ. Sci. Technol, 27, 1357-1363.

CARB (1991): "Proposed Reactivity Adjustment Factors for Transitional Low-Emissions Vehicles — Staff Report and Technical Support Document," California Air Resources Board, Sacramento, CA, September 27.

Carter, W. P. L. (1990): "A Detailed Mechanism for the Gas-Phase Atmospheric Reactions of Organic Compounds," Atm. Environ., 24A, 481-518.

Carter, W. P. L. (1991): "Development of Ozone Reactivity Scales for Volatile Organic Compounds", EPA-600/3-91/050, August.

Carter, W. P. L. (1993): "Development and Application of an Up-To-Date Photochemical Mechanism for Airshed Modeling and Reactivity Assessment," Draft final report for California Air Resources Board Contract No. A934-094, April 26.

Carter, W. P. L. (1994): "Development of Ozone Reactivity Scales for Volatile Organic Compounds," J. Air and Waste Manage. Assoc., 44, 881-899.

Carter, W. P. L., R. Atkinson, A. M. Winer, and J. N. Pitts, Jr. (1982): "Experimental Investigation of Chamber-Dependent Radical Sources," Int. J. Chem. Kinet., 14, 1071.

Carter, W. P. L., Dodd, M. C., Long, W. D. and Atkinson, R. (1984): Outdoor Chamber Study to Test Multi-Day Effects. Volume I: Results and Discussion. Final report, EPA-600/3-84-115.

Carter, W. P. L., W. D. Long, L. N. Parker, and M. C. Dodd (1986): "Effects of Methanol Fuel Substitution on Multi-Day Air Pollution Episodes," Final Report on California Air Resources Board Contract No. A3-125-32, April.

Carter, W. P. L. and R. Atkinson (1987): "An Experimental Study of Incremental Hydrocarbon Reactivity," Environ. Sci. Technol., 21, 670-679

Carter, W. P. L. and R. Atkinson (1989): "A Computer Modeling Study of Incremental Hydrocarbon Reactivity", Environ. Sci. and Technol., 23, 864.

Carter, W. P. L., and F. W. Lurmann (1990): "Evaluation of the RADM Gas-Phase Chemical Mechanism," Final Report, EPA-600/3-90-001.

Carter, W. P. L., and F. W. Lurmann (1990): "Evaluation of the RADM Gas-Phase Chemical Mechanism," Final Report, EPA-600/3-90-001.

Carter, W. P. L. and F. W. Lurmann (1991): "Evaluation of a Detailed Gas-Phase Atmospheric Reaction Mechanism using Environmental Chamber Data," Atm. Environ. 25A, 2771-2806.

Carter, W. P. L., J. A. Pierce, I. L. Malkina, D. Luo and W. D. Long (1993a): "Environmental Chamber Studies of Maximum Incremental Reactivities of Volatile Organic Compounds," Report to Coordinating Research Council, Project No. ME-9, California Air Resources Board Contract No. A032-0692; South Coast Air Quality Management District Contract No. C91323, United States Environmental Protection Agency Cooperative Agreement No. CR-814396-01-0, University Corporation for Atmospheric Research Contract No. 59166, and Dow Corning Corporation. April 1.

Carter, W. P. L, D. Luo, I. L. Malkina, and J. A. Pierce (1993b): "An Experimental and Modeling Study of the Photochemical Ozone Reactivity of Acetone," Final Report to Chemical Manufacturers Association Contract No. KET-ACE-CRC-2.0. December 10.

Carter, W. P. L., J. A. Pierce, D. Luo and I. L. Malkina (1993c): "Environmental Chamber Studies of Maximum Incremental Reactivities of Volatile Organic Compounds," Submitted to Atmospheric Environment, November 23.

Carter, W. P. L., D. Luo, I. L. Malkina, J. A. Pierce, W. D. Long, and D. Fitz (1995a): "Environmental Chamber Studies of Atmospheric Reactivities of Volatile Organic Compounds. Effects of Varying Chamber and Light Source", March 26.

Carter, W. P. L., D. Luo, I. L. Malkina, and D. Fitz (1995b): "The University of California, Riverside Environmental Chamber Data Base for Evaluating Oxidant Mechanism. Indoor Chamber Experiments through 1993," Report submitted to the U. S. Environmental Protection Agency, EPA/AREAL, Research Triangle Park, NC., March 20..

Chang, T. Y. and S. J. Rudy (1990): "Ozone-Forming Potential of Organic Emissions from Alternative-Fueled Vehicles," Atmos. Environ., 24A, 2421-2430.

Croes, B. E. et al. (1993): "Southern California Air Quality Study Data Archive," Research Division, California Air Resources Board.

Dasgupta, P. K, Dong, S. and Hwang, H. (1988): "Continuous Liquid Phase Fluorometry Coupled to a Diffusion Scrubber for the Determination of Atmospheric Formaldehyde, Hydrogen Peroxide, and Sulfur Dioxide," Atmos. Environ. 22, 949-963.

Dasgupta, P.K, Dong, S. and Hwang, H. (1990): Aerosol Science and Technology 12, 98-104

Dong, S. and Dasgupta, P. K. (1987): "Fast Fluorometric Flow Analysis of Formaldehyde," Environ. Sci. and Technol. 21, 581-588.

Gardner, E. P., P. D. Sperry, and J. G. Calvert (1987): "Photodecomposition of Acrolein in O_2-N_2 Mixtures," J. Phys. Chem. 91, 1922.

Jeffries H. E., K. G. Sexton, J. R. Arnold, and T. L. Kale (1989): "Validation Testing of New Mechanisms with Outdoor Chamber Data. Volume 2: Analysis of

VOC Data for the CB4 and CAL Photochemical Mechanisms," Final Report, EPA-600/3-89-010b.

Jeffries, H. E. and K. G. Sexton (1992): "The Relative Ozone Forming Potential of Methanol-Fueled Vehicle Emissions and Gasoline-Fueled Vehicle Emissions in Outdoor Smog Chambers," Annual Report for the Coordinating Research Council Project No. ME-1, August 30.

Johnson, G. M. (1983): "Factors Affecting Oxidant Formation in Sydney Air," in "The Urban Atmosphere -- Sydney, a Case Study." Eds. J. N. Carras and G. M. Johnson (CSIRO, Melbourne), pp. 393-408.

Lurmann, F. W., H. H. Main, K. T. Knapp, L. Stockburrger, R. A. Rasmussen and K. Fung (1992): "Analysis of Ambient VOC Data Collected in the Southern California Air Quality Study," Final Report to California Air Resources Board Contract No. A382-130; Research Division, Sacramento, CA, February.

Lurmann, F. W., M. Gery, and W. P. L. Carter (1991): "Implementation of the 1990 SAPRC Chemical Mechanism in the Urban Airshed Model," Final Report to the California South Coast Air Quality Management District, Sonoma Technology, Inc. Report STI-99290-1164-FR, Santa Rosa, CA.

Meyrahn, H., J. Pauly, W. Schneider, and P. Warneck (1986): "Quantum Yields for the Photodissociation of Acetone in Air and an Estimate for the Life Time of Acetone in the Lower Troposphere," J. Atmos. Chem. $\underline{4}$, 277-291.

Russell, A. G. (1990): "Air Quality Modeling of Alternative Fuel Use in Los Angeles, CA: Sensitivity of Pollutant Formation to Individual Pollutant Compounds," the AWMA 83rd Annual Meeting, June 24-29.

Tuazon, E. C., R. Atkinson, C. N. Plum, A. M. Winer, and J. N. Pitts, Jr. (1983): "The Reaction of Gas-Phase N_2O_5 with Water Vapor," Geophys. Res. Lett. $\underline{10}$, 953-956.